Safe Bunkering of Hydrogen-Fuelled Ships: Accounting for the Effects of DDT

Jørgen Nedrebø
University of Bergen

June 1, 2022

A thesis in partial fulfilment of the requirements for the degree of *Master of Science* in the subject of Physics; Process Safety Technology

Acknowledgements

First, I would like to thank my supervisor, Helene Hisken, for her guidance on the topic of hydrogen explosion, help with challenges related the FLACS software, detailed discussions, completely feedbacks and in general always available when I needed assistance.

I also want to thank my co-supervisiors, Bjørn J. Arntzen and Melodia Lucas Pérez, for meetings and their feedback on my work. Furthermore, I would express my gratitude to Gexcon AS for their hospitality by giving me an own desk at the office and for helping me with the FLACS software.

Finally, I would like to thank my fiancee, family and friends for their support and patience during my work of this thesis.

Bergen, June 2022

Jørgen Nedrebø

Abstract

Hydrogen will play an important role in the transition from today's use of conventional fuels to an energy system with net-zero emissions. IMO *(International Maritime Organization)*, is responsible for the safety and security of shipping and has a target of reducing greenhouse gas emission in the maritime sector by at least 50 %. Hence, hydrogen could be the dominant energy carrier for the future. However, it is not straightforward to replace conventional fuels with hydrogen, as the safety-related properties of hydrogen require alternative considerations and solutions. Compared to conventional fuels used in the maritime sector, hydrogen mixtures with air has a significantly wider flammable range, a very low minimum ignition energy, is significantly more reactive, and has a propensity to undergo deflagration-to-detonation transition (DDT).

This thesis is built on the scenarios explored in Johanne C. Jakobsen's master thesis from 2021 *"Towards a regulatory framework for the use of liquid hydrogen as a fuel for ships: Critical analysis of the prescriptive requirements for bunkering operations"*. In her thesis, Jakobsen conducted a critical analysis of the prescriptive requirements for bunkering operations of liquid hydrogen on ships. By using Jakobsen's scenarios, hypothetical cases of accidental release of liquid hydrogen and subsequent ignition during bunkering operations, was investigated. The analysis focuses on the potential for flame acceleration, overpressure generation and potential for DDT to occur. The analysis is performed with the consequence model FLACS.

Further, three hypothetical accident scenarios of a realistic port area, with different congestion levels, were simulated to study the potential for generating significant overpressures and DDT. The results from the simulations showed that all the cases achieved low overpressure and no sign of DDT. However, the number of investigated scenarios in the present work was limited, so this is not necessarily a general conclusion. The thesis includes suggestions for scenarios that should be explored in future studies.

To support the discussion of the hypothetical accident scenarios, two experimental campaigns are used to validate FLACS for this particular application. The applicability of FLACS to predict flame acceleration, overpressure generation and potential for DDT in geometries relevant for bunkering operations (large-scale and low degree of confinement) is analysed. The flame acceleration process in the experiments was not exactly reproduced in the simulations. However, the analysis showed that FLACS predicted the overpressure and the possibility of DDT with acceptable accuracy.

Abbreviations

AIT	Auto-Ignition Temperature
COP26	The 2021 United Nations climate change conference
CFD	Computational Fluid Dynamics
DDT	Deflagration-to-Detonation Transition
DDTLS	Detonation Length Scale, LSLIM/λ
DNS	Direct Numerical Simulation
DPDX	Spatial Pressure Gradient (Normalized)
GH2	Gaseous Hydrogen, or Compressed Hydrogen
GHG	Greenhouse Gases
FLACS	Consequence Model
IEA	The International Energy Agency
IGF Code	The International Code of Safety Using Gases or Other Low-Flashpoint Fuels
IMO	International Maritime Organization
LFF	Low Flash Point Fuel
LFL	Lower Flammability Limit
LH2	Liquid Hydrogen
LNG	Liquid Natural Gas
LPG	Liquid Petroleum Gas
MEPC	The IMO Marine Environment Protection Committee
MESG	Maximum Experimental Safe Gap
MIE	Minimum Ignition Energy
QD	Quenching Distance
QRA	Quantitative Risk Assessment
RANS	Reynolds-Averaged Navier-Stokes
VCE	Vapor Cloud Explosion
UFL	Upper Flammability Limit

Contents

1 Introduction and motivation

1.1 Background

Since the 1990s, the UN has been working with each country in the world and how they can increase their use of energy from renewable. At the time, climate change has since changed to a global priority, not a fringe issue which it was before. The Paris Agreement from 2015 set a goal to limit the temperature increase due to global warming to less than 2 degrees Celsius, and preferably to a maximum of 1.5 degree Celsius. This was the first universal and legal agreement about global climate change [1].

In November 2021 in Glasgow, the UN arranged a new climate change conference, COP26 (Conference on the Parties), for world leaders, ministers, but also representatives from civil society, business and international organizations. The main goal from the COP26 is to *"secure global net zero by mid-century and keep 1.5 degrees within reach"* [2]. To achieve this goal, all countries have to [2]:

- Accelerate the phase-out of coal.
- Curtail deforestation.
- Accelerate the switch to electric vehicles.
- Encourage investment in renewables.

Hydrogen is foreseen to play as an energy carrier in the transition to an energy system which will be net-zero emissions within 2050, and limit the increase of global warming. According to a report from Hydrogen Council [3], the use of clean hydrogen can avoid up to 80 gigatons of cumulative CO2 emissions before 2050. In sectors such as heating applications, long-range ground mobility and international travel, hydrogen will be critical for the enabling of a decarbonized energy system. One of the favorable features of hydrogen is that it can transport large amounts of energy via ships and pipelines [3].

1.2 Environmental challenges with maritime transport

The International Energy Agency (IEA) published a report in 2019 where they estimated that the global transport sector, i.e. road, aviation, marine and rail combined used 31 000 TWh in 2015 [4]. According to the IEA, this is around 14 % of the global greenhouse gases (GHG) emissions. In the maritime sector, international shipping accounts for 80 % of the fuel consumption. This is the most economical way to move long-distance freight, and represents most of the volume of the global physical trade. If nothing will change in the coming decades, IEA expects the volume to be more than tripled by 2050. The international shipping industry was in 2015 responsible for around 2.5 % of the global energy-related CO2 emissions. Furthermore, because of the massive use of diesel and heavy fuel oil, the maritime sector also has a large emissions of particulate matter and sulfur, which has detrimental effects on the air quality [4].

Today, the International Maritime Organization (IMO) is responsible for the safety and security of shipping, as well as the prevention of marine and atmospheric pollution from ships. IMO is a specialized agency of the UN, and supports the UN sustainable development goals. The IMO marine Environment Protection Committee (MEPC) investigates environmental issues under IMO's remit, which has increasingly strict requirements to limit sulfur emissions, air pollution and GHG emissions from ships. One measure for cutting emissions is to increase the use of fuels or energy sources with no carbon emissions, such as batteries or hydrogen [5].

IMO has a target of reducing the GHG emissions by at least 50 % in the maritime transport, which is the result of the Paris Agreement [6]. To achieve the goal of 50 % reduction it will be necessary with a strong initiative towards increased use of low-flashpoint fuel (LFF). LFF is "*a gaseous or liquid fuel with flashpoint below 60 C°for the primary fuel of a ship*" [7]. Hydrogen and several of the most relevant hydrogen-based fuels, such as methanol, ethanol and ammonia, are included in this category of fuels [7]. IMO regulate the transport and use of LFFs in specific codes: *(i) The IMO IGC Code (IMO,2016a)* is an international standard for the safe carriage of liquefied gases and *(ii) the IMO IGF Code (IMO, 2016b)* is an international standard for the safety of ships using low-flashpoint fuels, other than ships covered by

the IGC Code [7].

However, there are safety issues by using LFFs on ships. Compared to a release of conventional bunker oil, the loss of containment of LFF will be more likely to create an explosive atmosphere. In general, a transition towards increased use of LFFs is likely to be accompanied by an increase in the relative proportion of explosions, relative to fires, in the overall statistics of fuel-related losses in the maritime industry [8].

According to Skjold [9], hydrogen is arguably the most reactive and easily ignitable of all energy carriers ever considered for widespread use in society. It is therefore not straightforward to achieve and document the required level of safety for hydrogen systems. Furthermore, under specific conditions, hydrogen-air mixtures have a higher propensity to undergo deflagration-to-detonation-transition (DDT) than conventional fuels. A detonation represents a mode of flame propagation that is highly destructive, extremely challenging to design for, and not straightforward to mitigate after initiation (see Section 2.5 for further details on the DDT phenomenon). The probability that a DDT can occur after ignition of an accidental release of hydrogen must therefore be minimised.

1.3 Relevant accidents

The use of hydrogen as a fuel is relatively new in the process industry. However, there have been accidents related to handling hydrogen. This section will shortly describe three accidents which are relevant for this thesis.

Ohio, U.S, 2007
In January 2007, there was a hydrogen explosion at the Muskingum River Power Plant's in Ohio in the US. Under a delivery of hydrogen to their hydrogen system, a device failed and they got an accidental release of hydrogen. The hydrogen was ignited by an unknown source which created an explosion. The accident killed the person who drove the delivering truck, and injured 10 people who worked nearby. Additionally, buildings and materials got significant damage caused by the explosion. The investigation of the explosion pointed to a relief valve rupture disc premature failure [10].

Kjørbo, Norway, 2019
In June 2019, a Uno-X fuel station in Kjørbo in Norway had an accident related to a hydrogen explosion. This was a hydrogen station with on site production from electrolysis. The accident started with a release of hydrogen, before it developed into a major explosion which caused damage to loads onto highway, office building and fence. There were no injuries in the explosion. Gexcon AS investigated the accident, and said that the consequences of initial explosion only could be well understood if the cloud detonated (DDT) [1]. The investigation identified an error with a plug in a hydrogen tank in the high-pressure storage unit as the root cause of the accident. This provided a leakage of hydrogen out to the atmosphere, which created a hydrogen-air mixture. The investigation also said there would have been no leakage of hydrogen without a human error [6].

North Carolina, U.S, 2020
In April 2020, there was an explosion at the hydrogen fuel plant OneH2 in North Carolina, in the US. OneH2 was built in 2019, and was designed to distribute and produce hydrogen for semi trucks and forklifts. The hydrogen caused a major explosion, which made significant damage to buildings in the vicinity. Over 50 houses were impacted, and the majority of the houses got their windows blown out. There were no injuries, but people several miles away felt the blast. The accident is still under investigation by authorities, and there are therefore no public conclusions about any causes of the explosion [11].

1.4 Objectives

This master thesis entails a critical analysis of the applicability of the CFD tool FLACS to predict the flame acceleration, overpressure generation and potential for DDT after accidental release of liquid hydrogen and subsequent ignition during bunkering operations. The case is built on the scenarios explored by Johanne C. Jakobsen's thesis from 2021, where Jakobsen conducted a critical analysed of the prescriptive requirements for bunkering operations of hydrogen on ships. She suggested for further work [12]:

"*Further studies should explore more realistic conditions for bunkering operations, including conditions that may result in significant flame acceleration*

and DDT. Relevant geometrical configurations that could be represented in such studies include the elongated, semi-confined, and often congested space between the ship and quay (as well as under the quay), gangway and bunkering system, cable trenches, light poles and instrumentation boxes, forklift trucks and stack of pallets, containers (especially the space underneath or between containers), etc"

The main focus will be on the potential for achieving high explosion overpressures and DDT, and explore the sensitivity of the predicted consequences to various obstructions commonly present in quay areas and various positions of the flammable cloud.

The secondary objectives are:

- Validation of selected experiments, with a critical analysis of the applicability of FLACS to represent various physical phenomena.
- A literature study to identify recent experiments work involving hydrogen explosions in geometries relevant for bunkering operations (low degree of confinement and/or various degrees of congestion), with a particular focus on experiments where DDT was observed.

1.5 Thesis outline

The thesis consists of five chapters. Below is a brief overview of what the various chapters contain:

- Chapter 2: Description of the theory that is of importance in the context of the thesis.
- Chapter 3: Present potential and selected validation cases, including grid sensitivity and DDT studies.
- Chapter 4: Present and discuss the results from the simulations of the bunkering operations.
- Chapter 5: Conclusions and suggestions for further work.

2 Theory

This chapter presents the theory that is of importance in the context of the thesis. To begin with, this section will briefly discuss the properties of hydrogen with respect to safety. There are some well known challenges by using hydrogen as a replacement for conventional fuels. Furthermore, the consequence model FLACS is introduced, which is able to predict the consequences of flammable and toxic releases, gas and dust explosions, and jet and pool fires. Finally, deflagration and DDT phenomena are defined.

2.1 Properties of hydrogen

As discussed in Chapter 1, the maritime sector has several possible options for the challenge of finding a sustainable replacement for conventional fuels. One of the alternatives is hydrogen. However, there are some safety challenges associated with hydrogen. When hydrogen is used as a fuel on ships, the IGF code states that the safety level shall correspond to that which can be achieved with conventional fuels. The IGF code §3.2.1 specifies [7]:

"The safety, reliability and dependability of the systems shall be equivalent to that achieved with new and comparable conventional oil-fuelled main and auxiliary machinery"

Safety challenges of hydrogen

Two of the main challenges with hydrogen are storage and transportation. Gaseous hydrogen (GH2) is normally stored and transported at considerably higher pressure (up to 700 bar), compared to conventional energy carriers like propane (30 bar), natural gas (260 bar) and liquid fuels which just need atmospheric pressure in the tank space [12]. There are significant challenges as a result of the high storage pressure considering the prevention of loss of containment, which can be caused by component or material failure. Boiling point is another challenge by storing and transporting hydrogen. Liquid hydrogen (LH2) has a low boiling point (-253 °C), much lower than the other conventional fuels, such as LNG and fuel oils [16]. Therefore, LH2 demands special materials and a complex cooling system under storage and transport.

Table 1: *Properties of hydrogen and conventional fuels [13], [14],[15].*

Properties	**Hydrogen**	**Conventional fuels**
Density (kg/m^3)	0.087	Methane: 0.657 Propane: 493 Gasoline: 750 Diesel: 850
Laminar burning velocity (m/s)	3.25	Methane: 0.40 Propange: 0.46
Flammable limits (vol% fuel in air)	4 - 75	Methane: 5 - 15 Propane: 2 - 9.5
MIE (minimum ignition energy, mJ)	0.017	Methane: 0.28 Propane: 0.26
AIT (auto ignition temperature, °C)	580	Methane: 537 Propane: 493 Diesel: ca 220 Petrol: ca 250
Quenching distance (mm)	0.064	Methane: 2.03
MESG (Maximum experimental safe gap, mm)	0.29	Methane: 1.12 Propane: 0.92
Flash point (°C)	LH2: -253	LNG: -188 LPG: -104
Transport/storage pressure (bar)	700	LPG: 30 CNG: 260 Diesel/gasoline/ heavy oil: atmospheric pressure
Boiling point for transport/storage (°C)	LH2: -253	LNG: -162 Propane: -42
Detonation cell size (stoichiometric fuel-air mixture, mm)	19	Methane: 300 Propane: 70

Compared to other conventional energy carriers, a hydrogen-air mixture can be ignited by much weaker ignition sources and are flammable over a considerably wider concentration range. The lower flammability limit (LFL) of hydrogen (4.0 vol % in air) is similar to for instance methane (5.0 vol %) and propane (2.1 vol %). Furthermore, the upper flammability limit (UFL) for hydrogen (77 vol % in air) is much higher than for other conventional fuels. This implies that it is challenging to prevent the formation of explosive atmospheres [13].

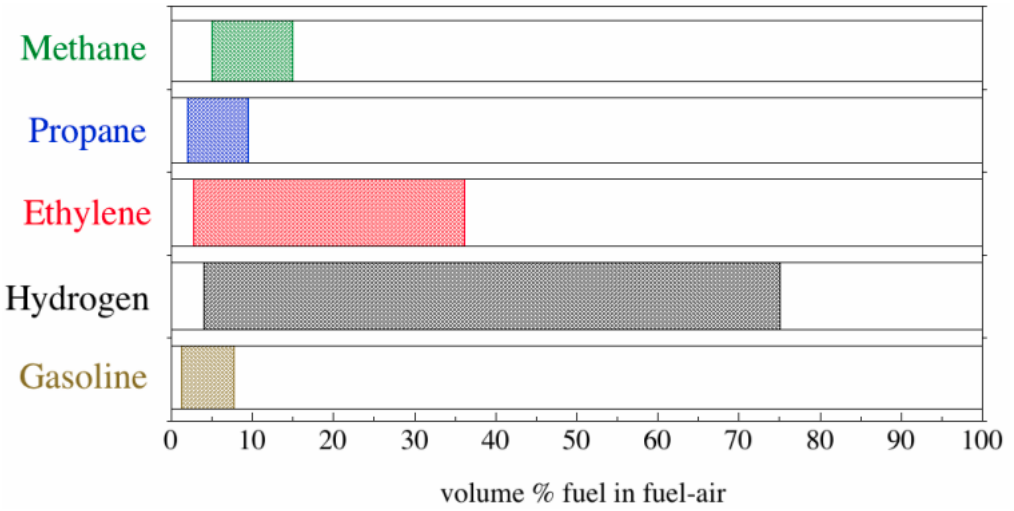

Figure 1: *The flammable limits for hydrogen and conventional fuels* [13].

Hydrogen has significantly smaller quenching distance (QD = 0,64 mm) and maximum experimental safe gap (MESG = 0,29 mm), in addition to very low minimum ignition energy (MIE = 0,017mJ) compared to conventional energy carriers. Furthermore, this entails several ignition sources that can be a potential hazardous ignition source for hydrogen-air mixtures, and therefore more difficult to prevent all ignition sources. Furthermore, a hydrogen-air mixture is significantly more reactive compared to conventional energy carriers. Hydrogen has higher maximum laminar burning velocity caused by high diffusivity and fast chemical kinetics [17].

If a cloud of hydrogen-air mixture gets ignited, there will be a turbulent combustion. This will give a significantly higher burning velocity than if there was a laminar combustion [17]. When the burning velocity is high,

there is a considerable risk of developing DDT if the right conditions are present [18].

Some favorable features of hydrogen
Compared to conventional fuels, hydrogen also has some characteristic properties that may be beneficial for safety. The first one is buoyancy, due to the low density of hydrogen, i.e. the density relative to air at the same temperature. This can reduce the consequences of accidental explosion by preventing the formation of large flammable clouds in unconfined congested areas. Therefore, natural convection in open geometries is advantageous for mitigation and prevention of hydrogen explosions [19].

If an accidental release of liquid hydrogen in atmospheric conditions occurs, it will rapidly evaporate because of a low boiling point (20K at atmospheric pressure). Since hydrogen is significantly lighter than air, it will instantly rise into the atmosphere. Compared to LNG, hydrogen has a higher vaporization which is advantageous in regards to safety, since the hydrogen will remain at ground level for a very short time [12].

Another beneficial property is that pure hydrogen flames do not produce soot, which gives less radioactive heat transfer compared to hydrocarbons. Finally, the auto-ignition temperature for hydrogen-air mixtures is similar to the auto-ignition temperature for conventional fuels [13].

2.2 Consequence modeling for risk assessment

In the process industry, safety is crucial for the environment, the economy and the people involved. An uncontrolled release of energy will be a significant hazard to people, the environment, society and the industry [20]. One of the major accidents in history was in Mexico City in 1984. It was a massive explosion from a tank with LPG (liquid petroleum gas), and over 600 people were killed and thousands injured. Just a few weeks after the explosion in Mexico City, a new accident happened in India. It was a release of toxic methyl isocyanate gas, which caused over 2000 deaths and over 200 000 injuries [21].

The examples above show the importance of risk assessment. The first step in a risk assessment is to identificate potential hazards and analyze the risk

for the system. A hazard can be defined as *"a chemical or physical condition that has the potential for causing damage to people, property, or the environment"* [19]. Risk can be defined as *"a measure of human injury, environmental damage or economic loss in terms of both the incident likelihood and the magnitude of the loss or injury"* [19]. Additionally, risk can be expressed as the product of frequencies and consequences. A frequency- and consequence analysis is an important part of the risk assessment. The result from the analysis can be put in a matrix, where the matrix will show if the risk is acceptable or not due to the requirements. Furthermore, if it is not acceptable, it is necessary to implement a reduction of risk measures and repeat the analysis [19].

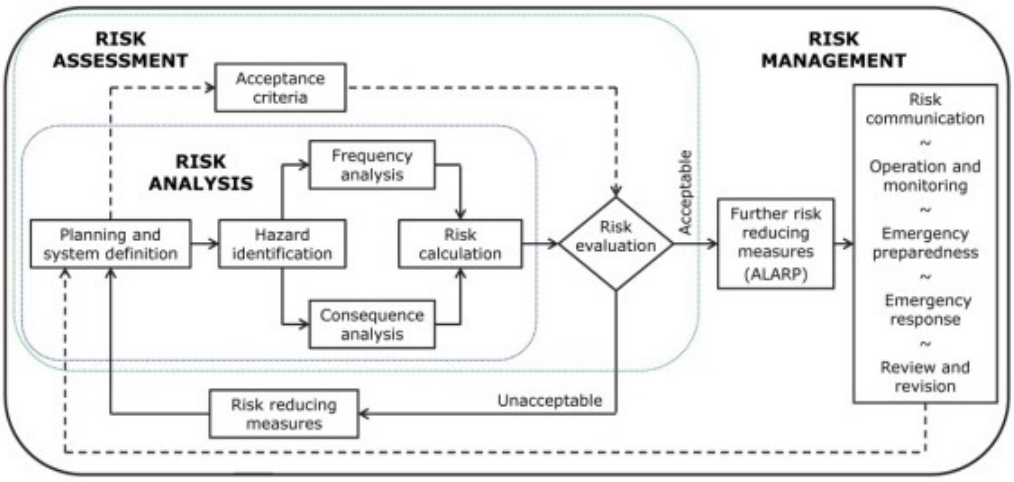

Figure 2: *Schematic representation of risk assessment, risk analysis and risk management* [9].

Furthermore, the strength of knowledge available for risk assessments of hydrogen safety is in constant development. Hydrogen systems do often address emerging technologies and inherently complex phenomena, which inherently limit the achievable level of accuracy in the risk assessment. According to Skjold [9], there is a substantial societal, technological and organizational challenge to document and achieve the required level of safety for hydrogen systems. A blind-prediction benchmark study from 2019, which was estimating the consequences of vented hydrogen deflagrations, disclosed lack of predictive capabilities for leading consequence models used for design of risk-reducing measures and consequence assessments [8].

2.3 The CFD tool FLACS

An essential part of the thesis is to simulate hydrogen explosions with the computational fluid dynamics (CFD) tool FLACS. In 1980, the Department of Science and Technology at Christian Michelsen Institute (CMI) started to develop the consequence model FLACS for simulating gas explosions offshore. Gexcon AS is currently the developer of FLACS and the tool is used for modelling and calculation for several safety aspects in the process industry. More specifically, FLACS predicts the consequences of flammable and toxic releases, gas and dust explosions, jet and pool fires and blast waves. The CFD tool FLACS uses numerical methods and algorithms to analyze and solve problems in fluid flow. For the present thesis, FLACS-CFD 21.1 has been used to perform hydrogen explosion scenarios involving flammable clouds generated by liquid hydrogen releases.

Computational fluid dynamics (CFD)

To predict the consequence of a gas explosion is critical for the safety of the process industry. There are different approaches. The first one build on empirical correlations and simplified physical considerations. Examples of models based on this are venting guidelines, complex empirical models and phenomenological models. These are all relatively quick and straightforward to use [22].

The second approach is computational fluid dynamics (CFD). CFD has frequently been used to perform quantitative risk assessments in the process industry. It is models which in different ways predict the consequences of potential accidents, including explosions and fires following a release of a flammable substance. CFD models are the most advanced models, where partial differential equations describing reactive fluid flow are discretized and solved on a computational grid [22].

The use of CFD models are restricted by the acceptable simulation time and computer time. Direct Numerical Simulations (DNS) can only simulate small systems and low Reynolds number flows. Additionally, the popularity of models that employ Large Eddy Simulation (LES) have increased in recent years. However, most commercial CFD tools still use turbulence models based on the Reynolds-averaged Navier Stokes equations (RANS) as a part of a quantitative risk analysis (QRA) [23].

Normally, CFD models use empirical and/or phenomenological sub-grid models to account for processes that are not resolved on the grid. In general the practically applicable computational cell sizes will be larger than the scales where the frame front, flow and geometry interact [24]. The thesis will follow the grid guidelines in the user manual of FLACS-CFD for the validation and simulations.

FLACS

For simulation of gas explosions, FLACS solves the Favre-averaged transport conservation equations for mass, momentum, enthalpy, mass fraction of fuel, mixture fraction, turbulence kinetic energy and the rate of dissipation of turbulent kinetic energy on a structured Cartesian grid. The equations are closed by invoking the ideal gas equation of state and the standard k - ϵ model for turbulence [23]. FLACS is a 3-dimensional (3D) software, where the velocity components are solved on a staggered grid and scalar variables, such as temperature, pressure and density, are solved on a cell-centered grid [25].

FLACS uses a distributed porosity concept to represent complex geometry. [25]. This means small objects are represented sub-grid, and large objects, like walls, are represented on-grid. In a simulation, the local confinement and congestion is represented by the porosity field, which allows sub-grid objects to contribute to turbulence generation, flow resistance (drag) and flame folding in the simulations [25].

Gexcon AS uses validation systematically for quality assurance of FLACS. They validate experiments, analytical solutions and real incidents for documenting best reliable estimates for the physical phenomena. That includes small scale cases, and large scale explosion and dispersion cases.

In the user manual of FLACS, there have been developed general guidelines for grids. FLACS uses a single-block Cartesian grid, which is cubic or rectangular grid cells defined by horizontal and vertical grid lines. There are certain guidelines for gas explosion simulations, which Gexcon AS renewed in the last version of the FLACS manual (Sep, 2021), based on validation against experimental results. It is essential to follow the guidelines to get the best results from simulations in FLACS [25].

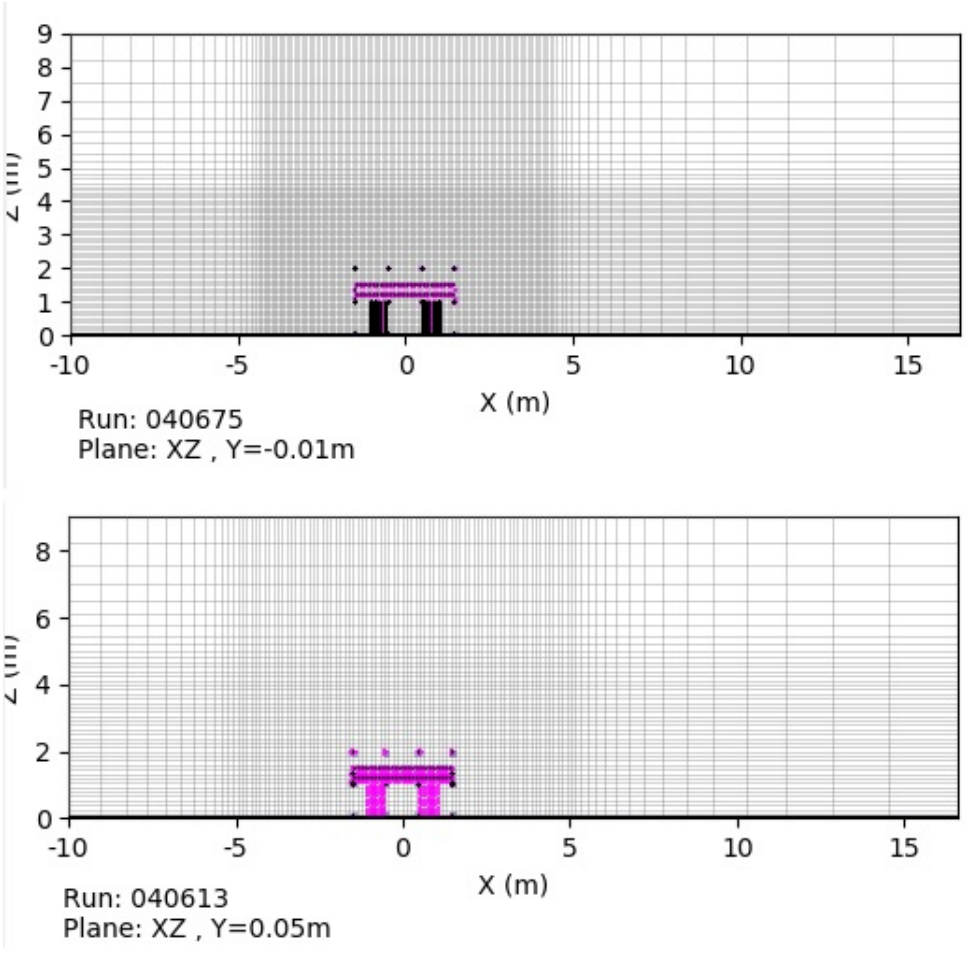

Figure 3: *An Illustration of how the porosity looks in FLACS. The examples are from validation case 1 in section 4.2, with a grid resolution of 0.075 m at the top and 0.13 m at the bottom.*

Below is a list over the most relevant guidelines for the present thesis [25]:

Core domain:

- Grid cells should be uniform and cubic, and they should be the same size in all dimensions.
- Include all areas where combustion takes place.
- The gas cloud should be resolved with at least 15 grid cells across its smallest dimension.

Total domain:

- Outside the core domain, the grid can be stretched to the domain boundaries using a stretch from one cell to the next that should not exceed 1.2.
- In directions where pressure wave propagation is of interest, the uniform grid spacing in the core domain should be maintained all the way to the targets in the direction of the external blast.
- For unconfined explosions, the distance from the core domain to the domain boundary should be the same in all dimensions.

For more details about FLACS and grid guidelines, see references "[25]".

2.4 Governing equations

The Navier-Stokes equations for conservation of mass, conservation of momentum and conservation of energy, express the fundamental physics principles in all fluid dynamics. This section will briefly describe the governing equations of fluid dynamics used for modelling gas explosions in the CFD tool FLACS. All the equations are from Hisken's PhD [24]:

Conservation of mass
The continuity equation describes the conservation of mass for a continuous system, and can be written as:

$$\frac{\partial}{\partial t}\left(\beta_v \rho\right) + \frac{\partial}{\partial x_j}\left(\beta_j \rho u_j\right) = \frac{\dot{m}}{V} \ , \tag{1}$$

where the source term on the right hand side accounts for mass that is added to or taken out of the simulation domain.

Conservation of momentum

The momentum equation is based on Newton's second law (F=ma) of motion for continuous fluids, and can be written as:

$$\frac{\partial}{\partial t}\left(\beta_v \rho u_i\right) + \frac{\partial}{\partial x_j}\left(\beta_j \rho u_i u_j\right) = -\frac{\partial}{\partial x_j}\left(\beta_v p \delta_{ij}\right) + \frac{\partial}{\partial x_j}\left(\beta_j \Omega_{ij}\right) + \frac{\partial}{\partial x_j}\left(\beta_v \theta_{ij}\right) + F_{o,i} + \beta_v\left(\rho - \rho_0\right) g_i \ , \tag{2}$$

where g_i is the ith component of the gravity vector, and the fluid is assumed to be isotropic.

Conservation of energy

The energy equation express the first law of thermodynamics, energy can neither be destroyed or created in an isolated system. The equation can be written as:

$$\frac{\partial}{\partial t}\left(\beta_v \rho h\right) + \frac{\partial}{\partial x_j}\left(\beta_j \rho h u_j\right) = \frac{\partial}{\partial x_j}\left(\beta_j \rho \mathcal{D}_{\text{th}} \frac{\partial h}{\partial x_j}\right) + \beta_v \frac{Dp}{Dt} + \frac{\dot{Q}}{V} \ , \tag{3}$$

where $\dot{Q}/V$ is a heat rate source term (e.g. accounting for heat transferred by radiation).

Conservation of species mass

If a fluid consists of several species in the same phase, the conservation of the mass fraction Y_F can be written as:

$$\frac{\partial}{\partial t}\left(\beta_v \rho Y_F\right) + \frac{\partial}{\partial x_j}\left(\beta_j \rho Y_F u_j\right) = \frac{\partial}{\partial x_j}\left(\beta_j \rho \mathcal{D}_{Y_F} \frac{\partial Y_F}{\partial x_j}\right) + \beta_v \dot{w}_F \ , \tag{4}$$

Conservation of mixture fraction

In simulations of gas explosion in FLACS, the mixture fraction denote the degree of mixing between the premixed fuel-oxidiser and the surrounding atmosphere. The conservation equation of the mixture fraction can be written as:

$$\frac{\partial}{\partial t}\left(\beta_v \rho \xi\right) + \frac{\partial}{\partial x_j}\left(\beta_j \rho \xi u_j\right) = \frac{\partial}{\partial x_j}\left(\beta_j \rho \mathcal{D}_{\xi} \frac{\partial \xi}{\partial x_j}\right) \ , \tag{5}$$

where $\mathcal{D}_\xi$ is the diffusion coefficient for ξ.

2.5 Regimes of combustion

An explosion can be defined in two ways. The first one focuses on a sudden release of a strong pressure wave into the atmosphere, a sudden outburst or a *"bang"*. The second definition is *"an exothermic chemical process that, when occurring at constant volume, gives rise to a sudden and significant pressure rise"*, and includes dust clouds, gases and solid explosives [13]. This part of the theory chapter looks closer at deflagration, detonation and the phenomenon deflagration-to-detonation-transition (DDT).

Deflagration

Deflagration can be described as a subsonic mode of combustion, where the chemical reactions occur more or less at constant pressure. The laminar burning velocity is normally less than 1 m/s for stoichiometric gaseous fuel/air mixtures at atmospheric conditions [26].

Laminar burning velocity is an experimentally determined property characterizing the propagation velocity of the flame normal to the flame front into the premixed reactants under laminar flow conditions [27]. Fuel mixture, equivalence ratio, pressure and temperature are all factors that impact the laminar burning velocity. For a combustible gas, experiments have shown that maximum laminar burning velocity normally occurs when the mixing ratio of fuel and air is close to the stoichiometric ratio, or just a bit over on the rich side. Stoichiometric ratio is when the ratio between fuel and air is accurately what is required for all the oxygen to transform all the fuel to H_20 and CO_2. If the fuel/air ratio moves away from the maximum laminar burning velocity point, either in richer or leaner direction, the velocity will systematically decrease. When it comes to hydrogen, the maximum laminar burning velocity occurs with the fuel/air ratio quite far over on the rich side. Furthermore, there are two finite limits where the mixture no longer will be able to propagate flame. The lower flammability limit (LFL) is where the fuel/air mixture is too lean to support a propagation flame front. On the other hand, the upper flammability limit (UFL) is where the mixture is too rich [13].

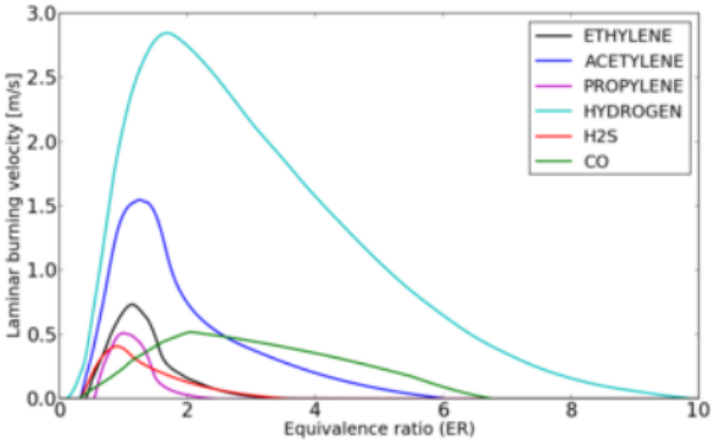

Figure 4: *Laminar burning velocity for hydrogen and other individual gas components* [25].

As the figure 4 shows, hydrogen has a significant higher laminar burning velocity than all the other gas components. The high velocity is caused by high diffusivity and fast chemical kinetics. However, combustions of a premixed cloud are rarely laminar, but turbulent. If a there is an accidental release of hydrogen, the cloud will be turbulent, not quiescent. In a turbulent combustion is the flame front folded and torn, not continuous like in a laminar combustion. The structure of the flame front is shown in figure 5. The effective surface area in a turbulent combustion can be sufficient larger than the nominal projeted area. This will, compared to the laminar value, gives turbulent burning velocities that in all probability is considerably high for a gas mixture in question [13].

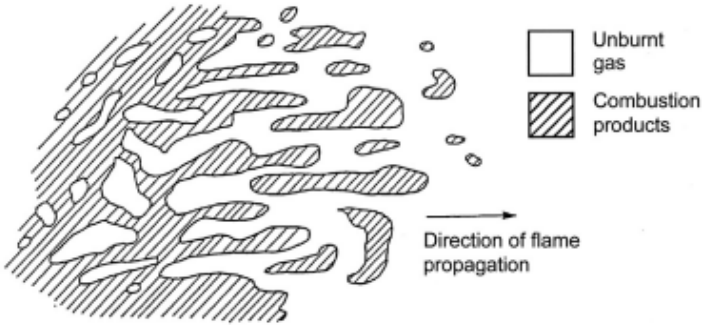

Figure 5: *The structure of the flame front in a turbulent premixed gas* [25].

Detonation

A detonation is defined as:

"*A supersonic combustion wave (e.i. the detonation front propagates into unburned gas at a velocity higher than the speed of sound in front of the wave)*" [28].

Therefore, the gas ahead of a detonation is undisturbed by the detonation wave. The pressure can be as high as 15-20 bar, and the detonation velocity is typically 1500 - 2000 m/s, in a fuel-air mixture at atmospheric pressure [28]. When a large amount of energy is released in a small volume, a detonation wave can be initiated directly [26].

Chapman and Jouguet developed the first acknowledged theory about the behavior of detonation, the CJ-theory. They treated the detonation wave as a discontinuity with infinite reaction rate. If the gas mixture is known, it is possible to calculate the detonation pressure, velocity etc, based on the one-dimensional wave theory from Chapman and Jouguet. However, the CJ-theory does not take into account any information about the chemical reaction rate. Zeldovich, Döring and von Neumann developed the theory by CJ-theory further by also accounting for the reaction rate. They described the wave of a detonation as a shock wave, followed by a reaction zone. The reaction rate determines the thickness of the reaction zone. The description of a flame zone with a finite thickness is the main difference between the ZND-model and the CJ-theory, since the ZND-model predicts the same detonation velocities and pressures [28].

It has been observed in experiments that the leading shock wave in a detonation consists of a cell pattern with curved shock segments. The detonation cell size, λ, is a characteristic length scale of one cell, which is used in prediction of DDT and as a measure of mixture sensitivity. However, there are some variations in the litterature about the experimental cell size data. The variations can be up to a factor of two, which indicates a large uncertainty. Since the detonation cell size not is a fundamental mixture property, it has to be validated experimentally. For hydrogen combustion, such as hydrogen-air mixture, the detonation cell size can be considered as a relevant scaling parameter [28].

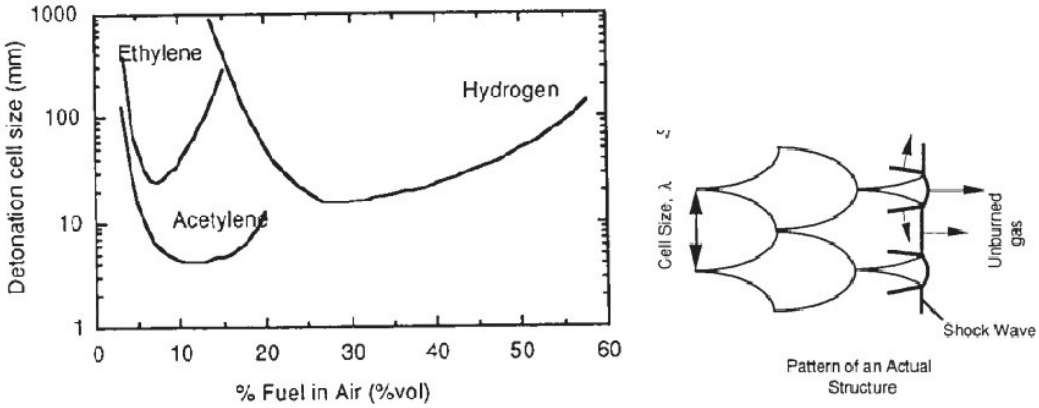

Figure 6: *Shows the pattern of a structure of a detonation front (right), and the detonation cell size versus fuel concentration for ethylene, acetylene and hydrogen in air (left)* [28].

Geometry conditions will limit the transmission and propagation of a detonation. A detonation cannot propagate in a pipe. Both the length scale of the geometry and the sensitivity of the gas mixture are limited conditions. By using the length scale of the geometry, which charactersing the reactivity of the mixture, the propagation and the transmission can be evaluated. Below are requirements for a successful propagation of a detonation [28]:

- Pipes:

$$D(diameter) > \lambda/3 \tag{6}$$

- Channels:

$$H(Height) > \lambda \tag{7}$$

Deflagration to detonation transition (DDT)
A definition of DDT is: *"When a deflagration becomes sufficiently strong, a sudden transition from deflagration to detonation can occur"* [28].

Mixtures that are very reactive, such as a hydrogen-air mixture, has the biggest chance for DDT to occur. DDT is very relevant for geometries like closed vessels and pipes. However, with today's evolving technology, it can be demanding to perform risk assessments due to an inherent lack of relevant experience. Turbulence is the key mechanism causing the flame acceleration in a pipe. In the combustion, the gas will burn and expand, which pushes the

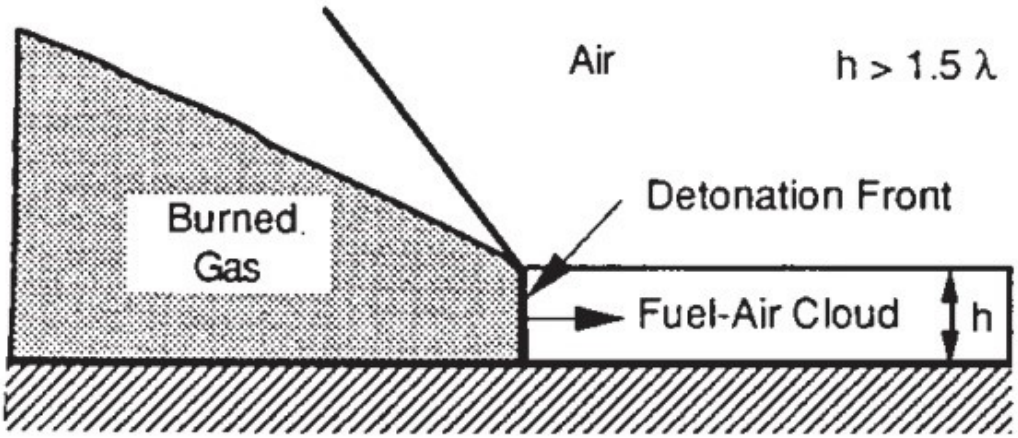

Figure 7: *Illustrate the limit in an unconfined fuel-air-cloud for propagation of detonation waves* [28].

unburned gas ahead. This unburned gas ahead of the flame front will create and then increase a turbulent boundary layer. The turbulence will boost the burning rate [28].

Bartknecht performed an experimental campaign that investigated flame velocities in pipelines in various scenarios. By using a pipe with either an open or closed end, he observed the flame velocities through the pipe. Bartknecht measured the highest flame speed when he ignited in the closed end while the other end was open. The gas ahead of the flame would in this case be pushed through the pipe and generate turbulence. The turbulence plays a key role causing the flame acceleration in a pipe. In the other case where both ends were closed, the flame accelerated fast in the beginning but after about halfway through, the flame startet to decelerate due to the closed end blocking the flow ahead of the flame [28].

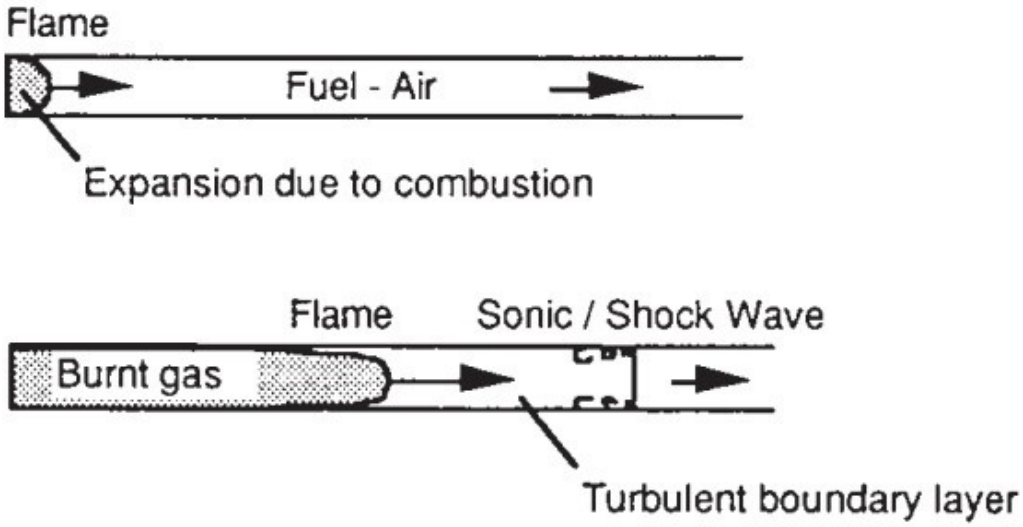

Figure 8: *Acceleration of the flame in a pipe* [28].

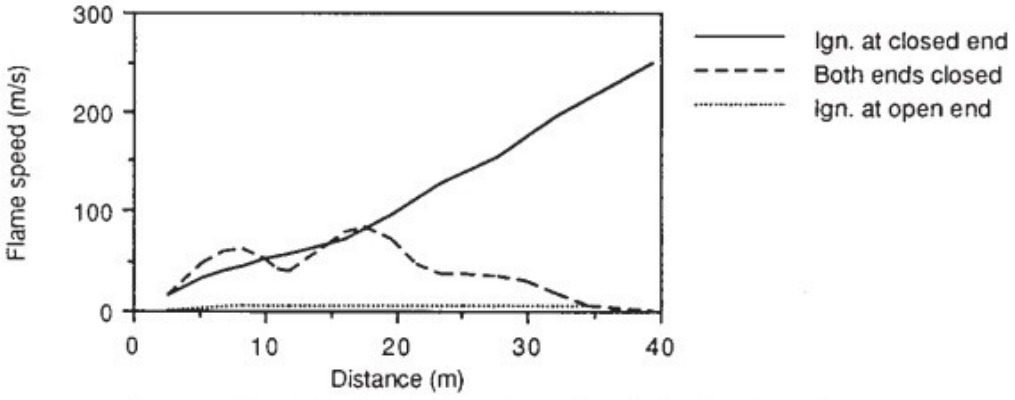

Figure 9: *Flame speed in a pipe (diameter = 1.4 m) with respectively ignition at closed end, ignition at open end and ignition with both ends closed, with methane-air mixture* [28].

DDT in FLACS

The CFD tool FLACS has no direct method for modeling DDT. However, Middha [22] and Middha & Hansen [29] developed a method for predicting the likelihood of DDT in FLACS occurring during a gas explosion simulation. Before, the method was to analyse when the front of the flame captured the pressure front. Hansen and Middha made a new model of predicting DDT in FLACS by including the parameters detonation cell size and geometric dimensions.

DPDX is a parameter which indicates when the flame front captures the pressure front and it is based on *"the normalised partial pressure gradient across the flame front"* [25]. In the FLACS user manual, they have included a figure showing which DPDX values indicate the likelihood for DDT. The figure is shown below:

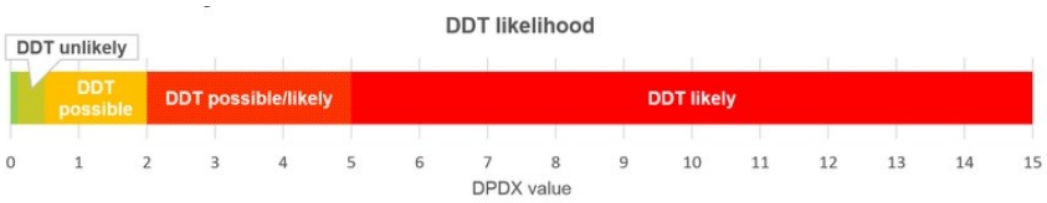

Figure 10: *An illustration of the likelihood of DDT with a DPDX value range from the FLACS manual* [25].

In the FLACS user manual, this is stated about DDT:
"*The DPDX value ranges indicated above are based on validation work that focuses mainly on confined hydrogen explosions: they may differ for other gases and degrees of confinement, and this is a topic of on-going research and validation efforts [25].*"

The figure 10 indicates that DDT is possible between the DPDX value of 0.5-2. Further, DDT goes from possible to likely between the DPDX value of 2-5. However, a DPDX value that indicates DDT is not enough to conclude whether a detonation will happen or not. According to the manual, it is also important to consider the area covered by the frame front compared to the detonation cell size of the gas. Additionally, DDTLS (DDT length scale ratio) can also be viewed from FLACS simulations. DDTLS compares the characteristic geometry of the present geometry to the detonation cell size

and illustrates whether a detonation wave can propagate easily. A DDTLS value of zero indicates no fuel, a value of more than 7 indicates easy propagation. In an unconfined situation, it is needed at least an area of 13 x 13 detonation cell sizes of gas cloud ahead of the fast flame front to be able to sustain a DDT [25]. The definition of DDTLS is the quotient of the characteristic geometrical dimension (LSLIM) divided by the detonation cell size (λ) [25]. The equation is showed in equation 8. LSLIM is the smallest distance between two blocked walls.

$$DDTLS = LSLIM/\lambda \tag{8}$$

Hisken did write this about the understanding of the parameters DPDX and DDTLS in her PhD [24]:
"*Assuming that the detonation cell size of a stoichiometric methane-air mixture is around 0.30 m, an area of 4 m x 4 m is needed for a detonation to propagate. A mixture of natural gas with air is somewhat more reactive than a pure methane-air mixture, so an area of 4 m x 4 m of DPDX exceeding 0.5 should be sufficient for suggesting that DDT is possible*".

3 Validation

"*Validation against experiments is the process of showing that a model reproduces measurements of specific physical parameters to satisfactory accuracy within its stated range of applicability*" (Ivings, M. J., et al., 2013) [30].

In this thesis, two experimental campaigns were simulated to analyze the applicability of FLACS to predict flame acceleration, overpressure generation and potential of DDT after weak ignition of a hydrogen-air mixture. Unconfined and large scale experiments were selected for validation.

Numerous gas explosion experiment campaigns with different fuels have been conducted. However, the number of large-scale hydrogen-air explosion experiments in unconfined conditions is rather limited. According to the report *"JIP FLACS 2011 and beyond"* [31], there are three experimental campaigns that could be relevant. It is a campaign from Shell [32] involving explosions in a congested rig, and a large scale campaign from BakerRisk [33]. Both were selected for validation in the present work, because they were most relevant for the bunkering operation cases presented in chapter 4. In addition, Shell completed a campaign in 2007, where a hydrogen release was ignited in simulated vehicle refuelling environment [31]. The last campaign is not considered further in this thesis.

3.1 Validation case 1

The first campaign that was simulated was an experimental study led by Shell B.V. The main objective for this study was to look at the potential consequences of explosions with high-pressure leaks from hydrogen vehicle refueling systems. The paper *"Experimental study of hydrogen explosion in repeated pipe congestion - Part 1: Effects of increase in congestion"* concluded [32]:
"*It is worth pointing out that these results are of sufficient quality to be used to develop models for the prediction of overpressure generated by explosion of hydrogen-air mixtures*"

The study is divided into two parts. The first part completed a series of hydrogen-air explosion experiments, where the level of congestion varied. The objective of the first part of the study was to [32]:

- *"Determine the effect of stoichiometric ratio on the overpressures measured with 4 arrays of pipes"* and
- *"Determine the effect of increasing the congestion on overpressures by increasing the number of layers of grids"*

In the second part of the study, they investigated the effect of hydrogen addition in methane-air clouds. The objective was to find out the amount of hydrogen that would give a large increase in the overpressure after an ignition [34]. The second part is not considered further in this thesis.

In the following, all results from the experiments, which show the effect of increasing the congestion and changing the equivalence ratio of the hydrogen-air cloud on the flame speed, explosion overpressure, and potential for DDT, will be compared to the results from the simulations. Grid sensitivity is also explored.

For more details about the experimental study, see references "Experiments part - 1" [32].

Description of the test facility

The congestion rig comprises a 3 m x 3 m x 2 m metal framework, structured so as to consist of eighteen 1 m^3 cubic units. Each grid comprised a number of 26 $\pm$ 1 mm diameter (nominal 1") bars spaced 125 mm apart.

Figure 11: *The congestion rig used in the experiments, congestion rig with 4-gates (left) and the rig with plastic sheet (right)* [32].

In the lower part of the layers of cells, the gates were inserted vertically. This is shown in figure 11. Additionally, there were up to 9 different lengths of

grids. The grids were organized within the rig to form concentric squares around the center cube. For the experiments, 4, 7 or 9 concentric squares of grids were used around the central 1m cube. The space between each grid was 0.15 cm.

The grids were placed horizontally in the top layers of cells. They were all the same dimensions, 3 m which is the length of the full frame, and one cell wide (1 m). 4 or 7 layers of grids were used for the experiments, with alternating layers running from left to right and top to bottom.

In the 9-gates experiments, a confinement wall was placed 1.7 m from the congestion rig, and 3.2 m from the ignition point.

The framework and grid arrangements were covered with a thin plastic film, similar to a cling film, from the outside. The film produced a near-airtight cover to the rig, which made it possible to fill the rig with a flammable fuel-air mixture. The ignition point was located in the center of the geometry, 0.5 m above the ground. It was an induction coil spark unit with a remote-control system.

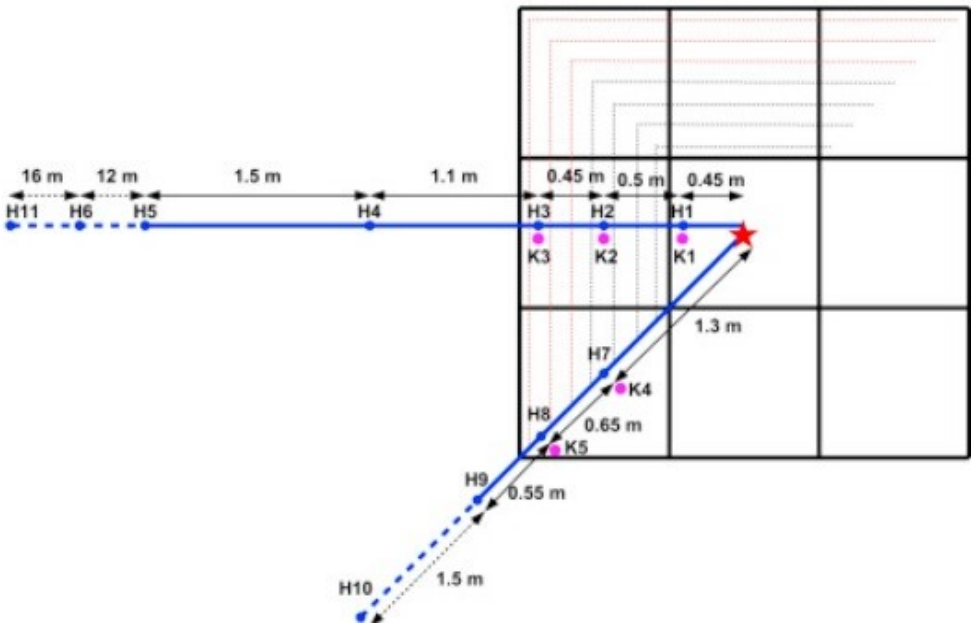

Figure 12: *The location of sensors for measuring in the experiments* [32].

Table 2: *Initial conditions for hydrogen-air experiments and simulations [32].*

Parameter	**4-01**	**4-02**	**4-03**	**4-04**	**4-05**	**4-06**	**7-07**	**9-08**
Number of gates	4	4	4	4	4	4	7	9
Stoichiometric ratio of mixtures on ignition	0.969	0.967	1.226	1.711	0.8	1.253	1.167	1.28
Free volume (m^3)	17.49	17.49	17.49	17.49	17.49	17.49	17.23	17.21
Wall present	No	No	No	No	No	No	No	Yes

In the experiments, two types of overpressure sensors were used:

- *Kulite Series ETK-345F-375M* 40 bara piezo-resistive transducers were used to measure higher overpressure, and all of them were located 0.5 m above the ground.
- *Brüel&Kjær 8103 hydrophones* were used to record lower overpressure. Most of the sensors were located 0.5 above the ground, except hydrophone 6 (1.2 m above) and hydrophone 11 (4.4 m above) due to topology.

The name of the tests and the simulations were divided into the number of gates they had in the test. All the tests with four gates start with the number "4", the test with 7 gates start with "7" and the test with 9 gates start with "9". For more details, look at table 2.

FLACS simulations

The FLACS geometry was based on that from an earlier simulation study, with some minor adjustments [22].

In all the simulations, the grid cells were uniform and cubicle. The grids were stretched away from the geometry, but not in the area where the main combustion happened. This is according to the guidelines in the FLACS User Manual [25]. Figure 13 shows the geometry as represented in the FLACS pre-prosessor CASD. All of the monitor points were in the x-direction, and therefore the grid in the x-direction is the least stretched. All the simulations were completed with the ambient temperature of 20 C°and initial atmospheric pressure of 1 bar, in quiescent conditions.

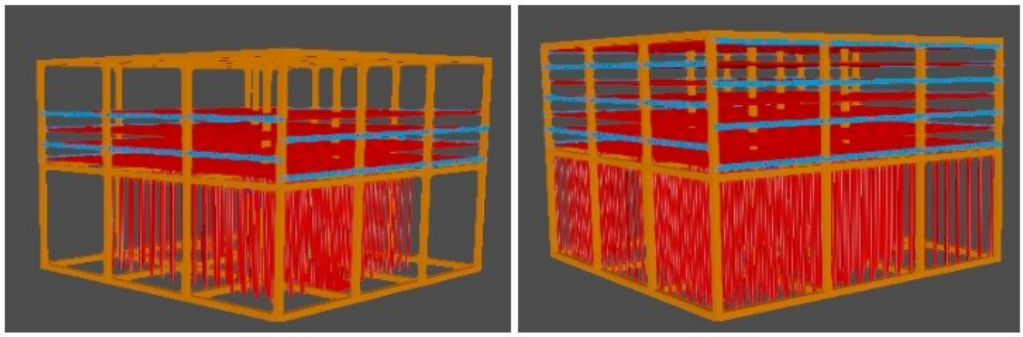

Figure 13: *3D views of the rig geometry, 4 gates (left), and 7 gates (right)* [32].

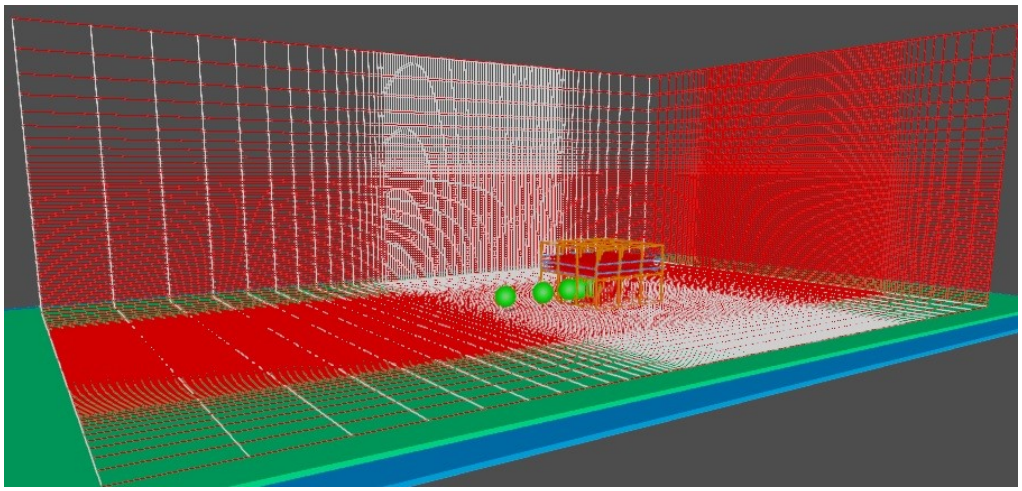

Figure 14: *Monitor points, the set-up for the geometry and the grid from the simulations in FLACS* [32].

Table 3: *An overview of the monitor points in the simulations [32].*

Monitor points	**Distance from ignition point (m)**	**Location**
H1	0.45	Inside rig
H2	0.95	Inside rig
H3	1.40	Inside rig
H4	2.50	Outside rig
H5	4.00	Outside rig
H6	16.00	Outside rig

The experiments were simulated with a grid resolution of either 0.13 m, 0.075 m or 0.05 m. The 0.13 m grid simulation had the largest grid resolution that fulfilled the guidelines in the FLACS User Manual [25] that require at least 15 grid cells across its smallest dimension. The simulation with 0.05 m grid is included because Prankul Middha used this resolution in his corresponding validation study [22]. In total, the simulations with 0.05 m grid domain contained around 6.8 million control volumes. Test 4-01 and 4-06 were not included in the validation study because they had very similar stoichiometric ratio to respectively test 4-02 and 4-03, and therefore expected to get similar results.

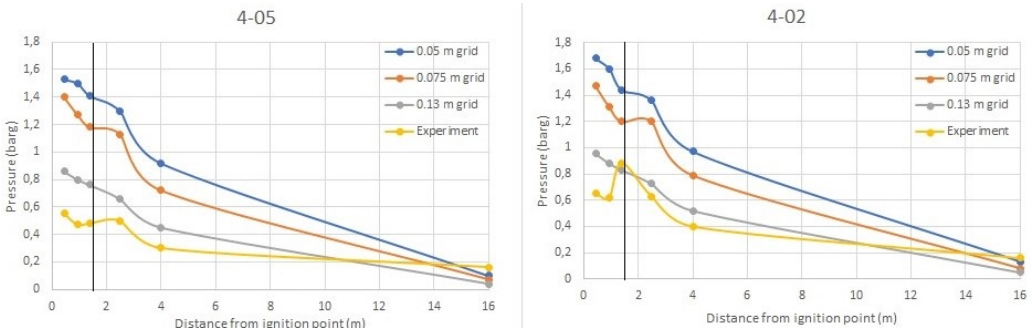

Figure 15: *Maximum ovepressure vs. distance from test 4-05 (left) with a stoichiometric ratio of 0.8 and test 4-02 (right) with stoichiometric ratio of 0.967. The black line indicates where the rig ends* [32].

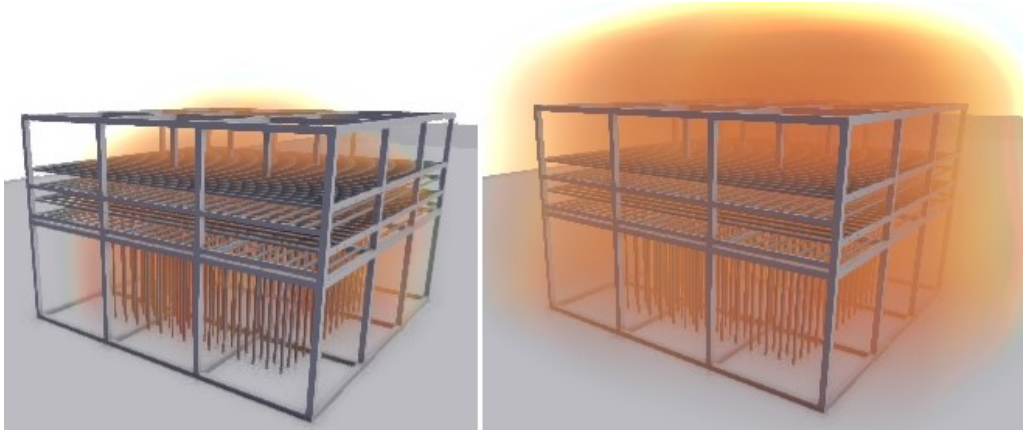

Figure 16: *Shows the combustion product mass fraction from the simulation of test 4-02 after respectively 0.043 and 0.045 s.*

Figure 15 shows results from tests 4-02 and 4-05, which both had a stoichiometric ratio below 1. The maximum overpressure from test 4-05 was less than 0.6 barg, and the overpressure decreased after monitor point 4 (outside the rig, 2.5 m from ignition point). The simulations had similar profiles as observed in the experiments, but in general higher overpressure immediately after ignition. The resolution with 0.13 m grid was roughly 0.2-0.3 bar higher than the experimental result after the ignition. This grid resolution resulted in the best agreement with the experimental results for test 4-02 and 4-05. Test 4-02 had a stoichiometric ratio of 0.967 which results in slightly higher pressures. Compared to test 4-05, the experiment result had a marked top in the overpressure with 0.88 bar at 1.4 m from the ignition point (monitor point 3), which is close to the end of the rig. This top does not exist in the simulations. The simulation with 0.13 m grid had the most similar overpressure results compared to the experiment. However, the simulation predicted over 0.3 bar higher overpressure after the ignition.

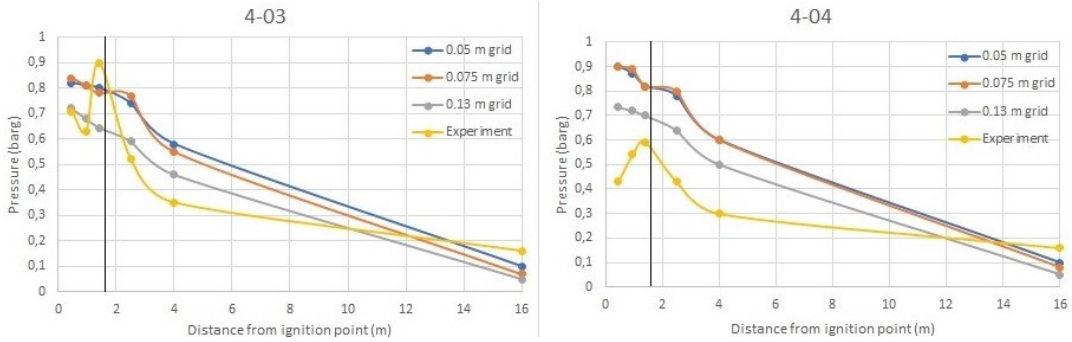

Figure 17: *Maximum ovepressure vs. distance results from from test 4-03 (left) with stoichiometric ratio of 1.226 and test 4-04 (right) with a stoichiometric ratio of 1.711. The black line indicates where the rig ends* [32].

The experimental results from 4-03 clearly had a marked increase in maximum overpressure at monitor point 3 (1.4 m from ignition point) with about 0.9 bar. There were no similar pressure increase at the end of the rig in the simulations, they had all the maximum overpressure at monitor point 1 (closest to the ignition point). Apart from the missing overpressure top, the simulation with the resolution of 0.13 m grid gave the best agreement with the overpressure result from the experiment.

Test 4-04 is a fuel-rich mixture with a stoichiometric ratio of 1.711. The experimental results show a lower overpressure compared to the 4-03 test, which was expected because of a stoichiometric ratio much higher than 1.

Further, the experimental results also had a marked pressure top at monitor point 3. The maximum overpressures vs. distance from the ignition point in the simulations were all decreasing slowly from monitor point 1. The simulation with 0.13 m grid was, as in test 4-02 and 4.05, closest to the overpressure results from the experiments.

Figure 18 shows the flame arrival time for the 4-gates tests at monitor point 1, 2 and 3. In general, the experiments used a shorter time to reach monitor point 1 (0.45 m from the ignition point) than the simulations. For test 4-03 (stoichiometric ratio of 1.226), it was over 20 ms in difference at each monitor point compared to the experiment arrival time. Tests 4-02 (stoichiometric ratio of 0.967) and 4-04 (stoichiometric ratio of 1.711) also showed a large deviation in flame arrival time, with around 10-15 ms in difference. The only simulation that had an almost similar arrival time profile compared to the experiment, was test 4-05, which was the test with the lowest stoichiometric ratio (0.8).

Figure 19 compares the flame speed for the 4-gates congestion simulations with the experiments. It it clear that the simulations achieve higher flame speeds than observed in the experiments at monitor point 1. The simulated flame speeds were between 45 - 100% higher than the experiments. At monitor point 3, the experiments achieved the highest flame speed (145-185 m/s). In general for the flame speed, the largest discrepancy between the experiments and the simulations was observed at monitor point 3. This must be seen in context with the increase in maximum overpressure in the experiments, which was at monitor point 3. Further, tests 4-02 and 4-05 has the highest flame speed for the simulations at monitor point 3, with a stoichiometric ratio of 0.967 and 0.8, respectively. Hence, the simulations that were stoichiometric, or close to stoichiometric on the lean side, achieved the highest flame speed.

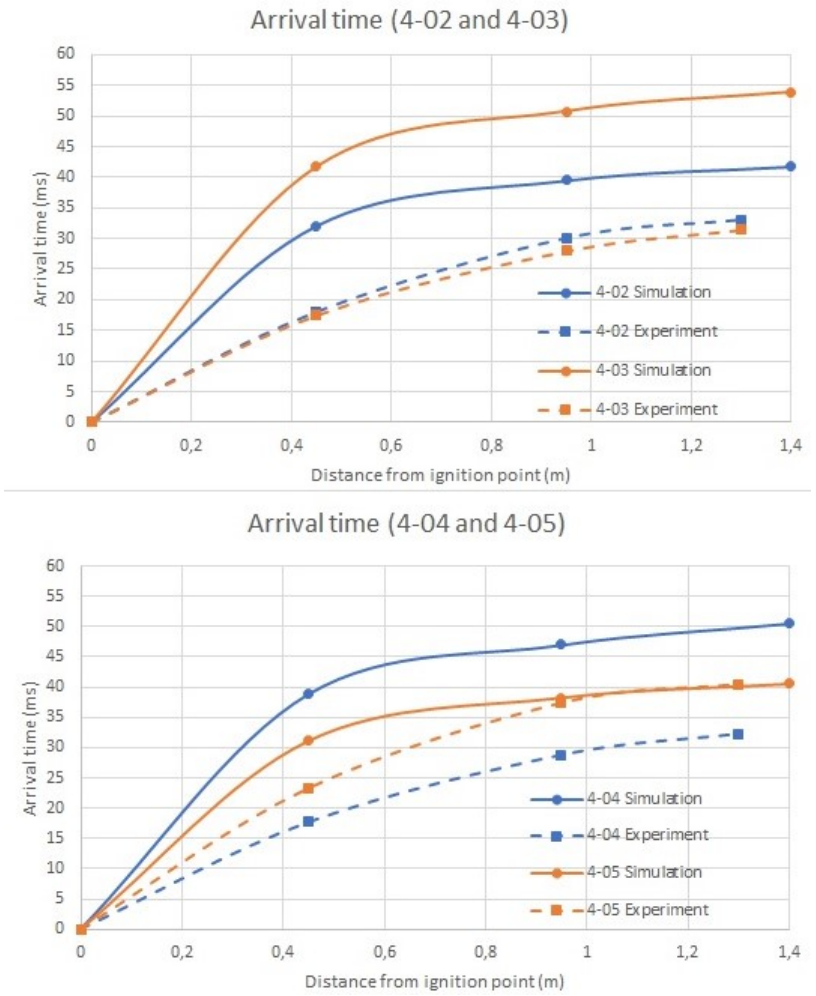

Figure 18: *The flame arrival time between the ignition point and monitor point 3 (1.4 m from the ignition point), for the simulations and the experiments at monitor point 1, 2 and 3. Tests 4-02, 4-03, 4-04 and 4-05 are included. The results are from the simulations with 0.13 m grid resolution. The experiment results end at 1.3 m from the ignition point.* [32].

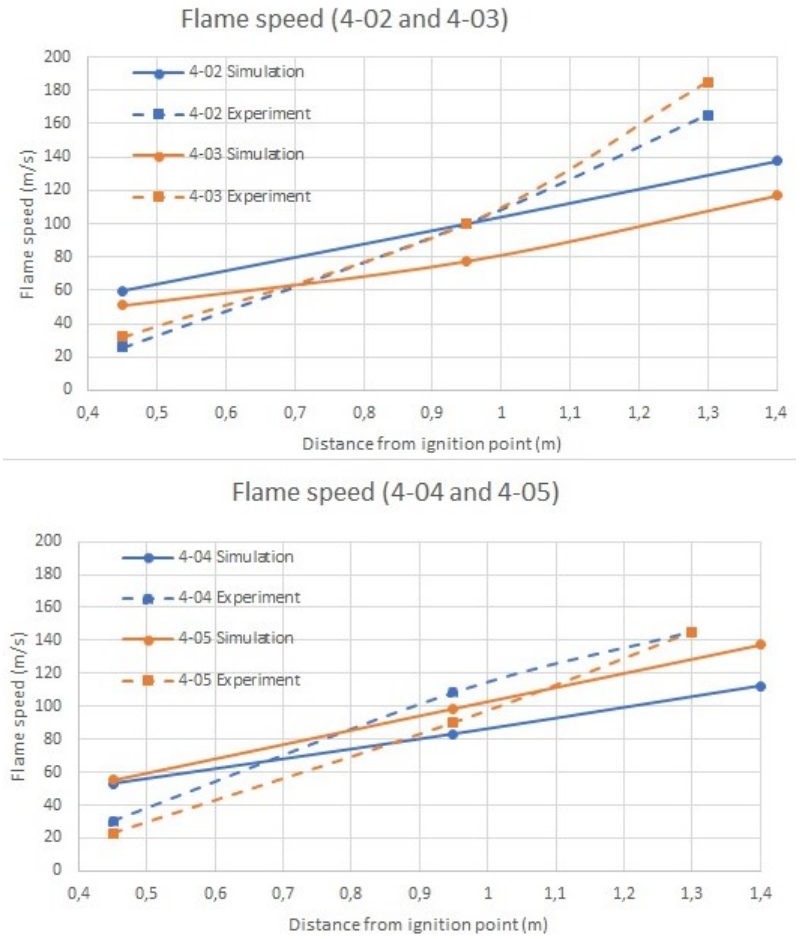

Figure 19: *The flame speed between monitor point 1, 2 and 3 in the simulations and the experimental for test 4-02, 4-03, 4-04 and 4-05. The results are from the simulations with 0.13 m grid resolution. The experiment results end at 1.3 m from the ignition point* [32].

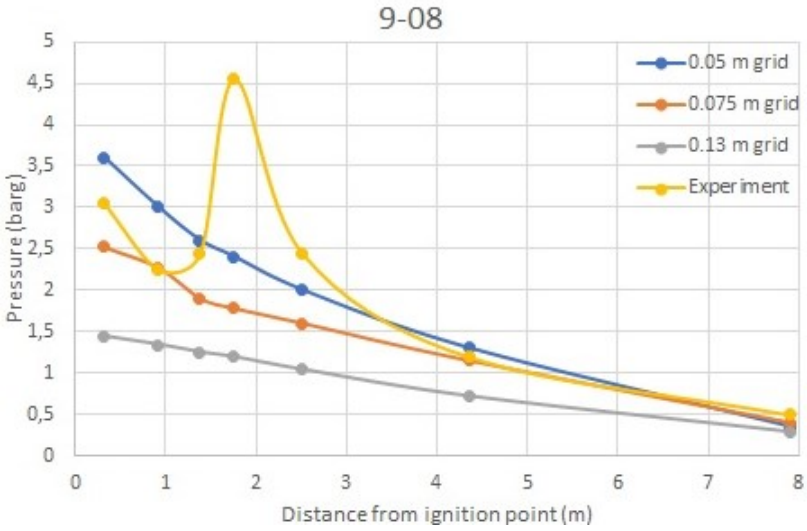

Figure 20: *Experiment and simulation result from test 9-08 with a stoichiometric ratio of 1.28, and a congestion rig with 9-gates. The black line indicates where the rig ends* [32].

In the experimental study, there were two tests that differ from the rest. Test 7-07 and 9-08 both have a higher number of gates in the rig. 7-07 has three added gates in the rig. Unfortunately, there was discovered a mistake in the simulations of test 7-07 with 7-gates congestion. Hence, all the results from test 7-07 have to be regarded as invalid. Due to limited time, the results from the simulations of test 7-07 are excluded from the thesis. Further, test 9-08 has a congestion rig with 9-gates. The experimental results show significant increase in overpressure at monitor point 4 of around 4.5 barg. This was not observed in any of the simulations. Apart from the behaviour at monitor point 3 in the experiment, the resolution of 0.13 m in the simulation results gives the most accurate predictions when compared to the results from the experiments.

Grid sensitivity study

The resolution of the 0.13 m grid was the largest recommended size of the grid for the geometry of this case, according to the guidelines in the FLACS User Manual [25]. In the tests with 4-gates congestion, the 0.13 m grid simulations resulted in the most accurate overpressure predictions compared to the experimental results. The simulation with 0.13 m grid resolution has

in general a bit higher overpressure than the experiment. Moreover, the overpressure increased in most of the experiments at monitor point 3. This was not observed in any of the simulations. Further, the simulation result from 9-gates congestion shows that the 0.075 m grid gave the best agreement with the experimental result.

Hence, the resolution of the 0.13 m grid was found to be the most accurate for 4-gates congestion. The simulations with finer grid size achieved in general a too high overpressure, especially close to the ignition point. Further, the resolution of the 0.075 m grid was found to be the most accurate for 9-gates congestion. Hence, these grid resolutions are used further in the validation study of this experiment.

Analysis of the overpressure and potential of DDT

The experimental study [32] investigated how the overpressure changed when the congestion level was increased. An increase from 4- to 7-gates gave a three times higher overpressure in the experiments. Further, the 9-gates achieved a overpressure up to two times higher than the 7-gates congestion level [32].

Table 4: *Essential results from the experiments and the simulations [32].*

Test	**Equivalence ratio**	**Max pressure experiment (barg)**	**Max pressure simulation (barg)**	**Max flame speed simulation (m/s)**	**Max flame speed experiment (m/s)**
4-02	0.967	0.95	0.88	138	165
4-03	1.226	0.72	0.90	117	185
4-04	1.711	0.74	0.60	112	145
4-05	0.8	0.86	0.55	138	145
9-08	1.28	3.05	4.55	-	-

Further, in the test with 9-gates congestion (9-08), the maximum overpressure in the experiment was observed just outside the rig, which suggests that a DDT may have occured as the flame front exited the rig [32]. Figure 21 shows the DPDX-value at 0.038 s after the ignition for the 9-08 simulation. The plot indicates that that the DPDX-value is at least 2. The DDTLS-value is significantly higher than 7, which indicates that DDT is possible. On the other hand, the LSLIM-value in the DDTLS equation 8 is a complex parameter to analyse. Since the test was not completely confined, the LSLIM-value is defined by the extent of the computational domain in FLACS. However, the analysis of DDT in simulation 9-08 shows that DDT is possible.

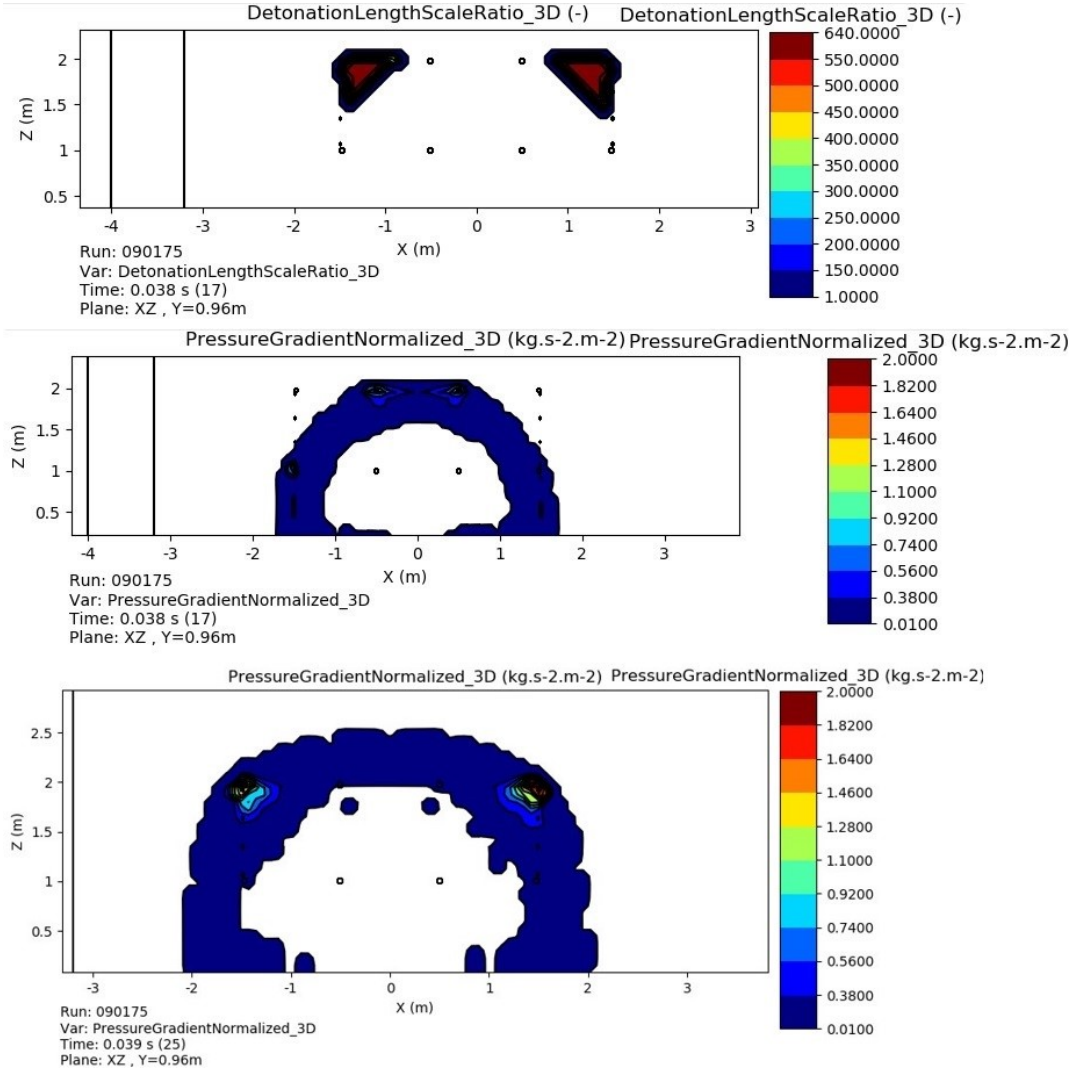

Figure 21: *Plot from the simulation for test 9-08 (9-gates congestion) of the DDTLS-value at 0.038 s. There are also plots of the DPDX-value after respectively 0.038 and 0.039 s. The DPDX is visualized to maximum 2. Flame propagation occurs from the middle of the geometry and towards all directions.*

Conclusions of validation case 1

- The grid sensitivity study showed that the largest recommended grid resolution (0.13 m) resulted in the most accurate results for the experiments with the lowest congestion level (4-gates congestion). When the congestion level was increased to 9-gates congestion, a finer grid (0.075 m) gave the most accurate results.
- The flame speed close to the ignition point is higher in the simulations compared to the experiments. This has to been seen in context with a higher overpressure in the same area for the simulations. Towards the end of the rig (monitor point 3), the flame speed in the experiments is higher than in the simulations. The flame acceleration process in the experiments is thus not exactly reproduced in the simulations.
- The simulation of 9-08 was the only test with unexpected result compared to the experiment. This was the test with the highest degree of congestion, and a wall located close to the rig. The experiment achieved a considerable higher overpressure, especially towards the end of the rig.
- Possible reasons for deviations between experimental and simulated results:
  - Inaccuracies in the modelling approach.
  - Minor deviations in geometric details, due to some interpretation from the illustrations in the paper.
  - How FLACS accounts for the effect of varying concentrations on the reactivity of the mixture [35].

3.2 Validation case 2

In 2017, Baker Engineering and Risk Consultants performed the experimental campaign *"Ammonia and Hydrogen Vapor Cloud Explosion Testing"* [33]. They wanted to look at the potential blast loading resulting from an accidental and unconfined vapor cloud explosion. There have been doubts and questions about whether hydrogen and/or ammonia actually pose a vapor cloud explosion (VCE) hazard. For ammonia, it has been discounted as a VCE hazard due to the low laminar burning velocity and the perceived difficulty in igniting an ammonia-air mixture. Hydrogen has also been discounted as a VCE hazard, because it is difficult to form a sufficiently large enough explosible cloud. That is due to the low MIE hydrogen has, which makes it likely that a release of hydrogen ignites before the cloud has reached a sufficient volume. Additionally, buoyancy will cause a hydrogen release to rise into the atmosphere, which makes it likely to not be an explosive and large enough cloud to make a VCE.

BakerRisk studied the pressure, flame speed, VCE and DDT after hydrogen explosions in their experimental campaign. Validating FLACS against these experiments will be useful later in the thesis when analyzing of the potential DDT in the bunkering operations. Additionally, a grid sensitivity and an investigation of the potential of DDT in FLACS is performed at the end of the section.
For more details about the experiment from BakerRisk, see reference [33].

Description of experiments

The test rig for the hydrogen tests were composed of 16 cubes, as seen in figure 22, where all were the same size, 1.8 m x 1.8 m. In total, the rig was 14.6 m x 3.7 m x 1.8 m. Each cube contained an arrangement of 45 vertical circular tubes. The diameter of the tubes was 6 cm, which gives a pitch-to-diameter ratio of 4.5. The volume blockage and provided area blockage ratios were respectively 4.1 % and 22 %. There were no walls in the experiments. The ignition point in the experiments was located in the center of the rig and 0.3 m above ground level. The mixture was ignited by using an electrochemical match. A sketch and a photograph of the rig are shown in figure 22. The fuel was injected into the rig by six venturis. Additionally,

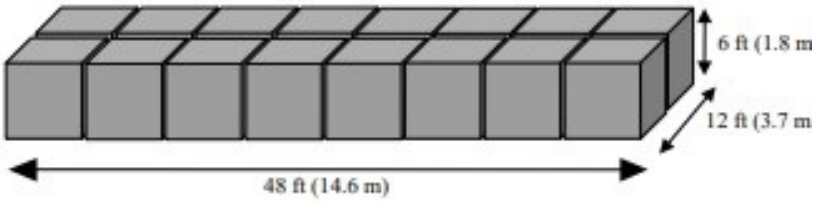

Figure 10. Schematic of Hydrogen Test Rig

Figure 22: *Sketch of the hydrogen test rig and a photograph of the hydrogen rig test* [32].

Table 5: *Hydrogen fuel concentration (%) and equivalence ratio for each test [33]*

Test	**Concentration (%)**	**Equivalence Ratio**
H01	16.0	0.44
H02	18.1	0.51
H04	20.1	0.58
H05	22.2	0.66

there was one fan attached to the top of each cube to mix the mixture. The concentration of hydrogen for the tests was 16 %, 18.1 %, 20.1 % and 22.2 %. All the mixtures were lean, with a stoichiometric ratio varying between 0.44 and 0.66 [33]. See table 5 for all the details.

FLACS simulations

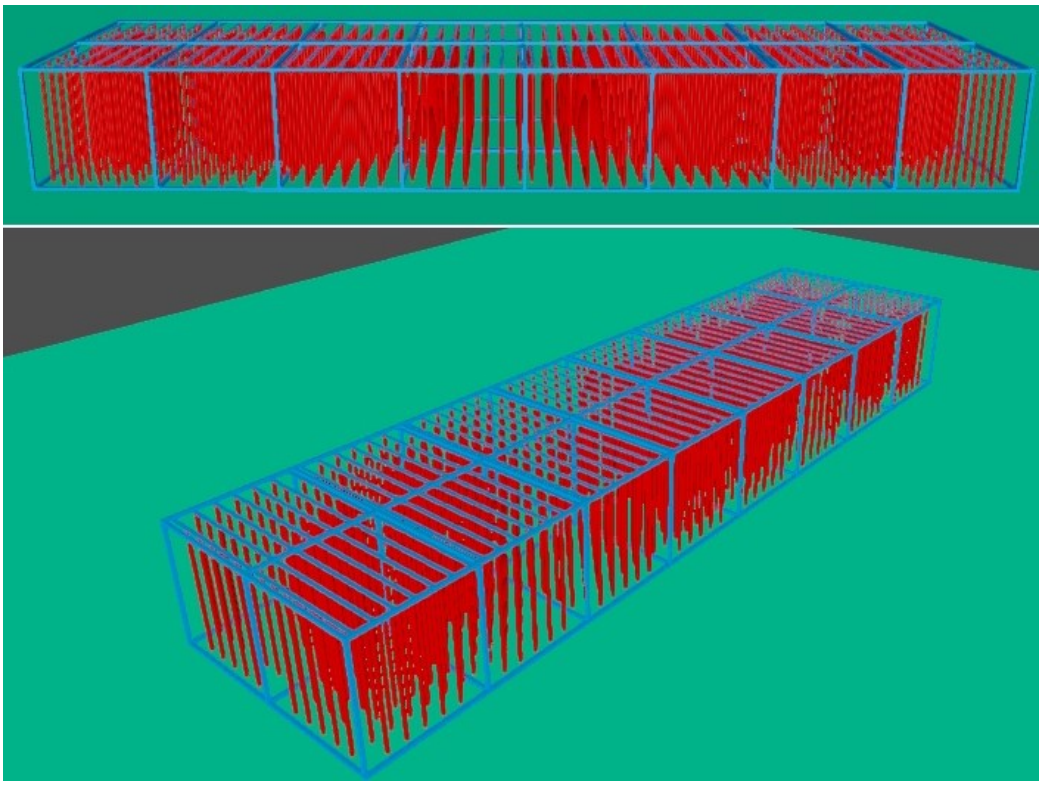

Figure 23: *3D views of the rig in the simulations.*

All the simulations were completed with uniform and cubicle grid cells in the simulation domain where the combustion happened. The grids were stretched away from the geometry, mostly in the z- and y-directions. The monitor points were located along the x-axis and around 0.3 m above ground level, as in the experiment. In total, the simulations domain with a 0.075 m grid resolution contained around 2250000 control volumes. All the simulations were completed with an ambient temperature of 20 °C and initial atmospheric pressure of 1 bar, in quiescent conditions. Additionally, the initial turbulence parameters were set to zero.

The experiments were simulated with grid resolutions of respectively 0.12 m and 0.075 m. The 0.012 m grid simulation had the the coarsest grid resolution that fulfills the guidelines from the FLACS user manual. The

Table 6: *An overview of the monitor points in the simulations [32].*

Monitor points	**Distance from ignition point (m)**	**Location**
1	3.00	Inside rig
2	4.00	Inside rig
3	5.20	Inside rig
4	6.90	Inside rig
5	9.50	Outside rig
6	11.90	Outside rig

guidelines require at least 15 grid cells across its smallest dimension. The first test (H01) was not included in the validation study because of expected low maximum pressure and low potential of DDT. The grid is shown in figure 24.

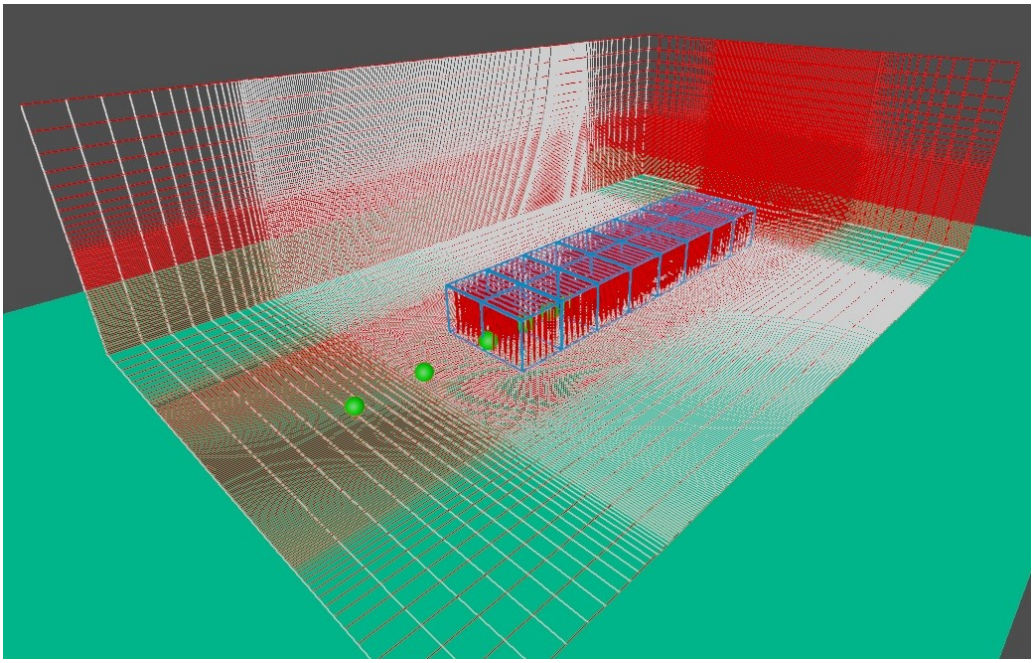

Figure 24: *Illustrate the grid and the monitor points in the simulations in FLACS.*

Figure 25 shows the maximum overpressure for test H05 from the experiment and the simulations. Both grid resolutions produced higher overpressures closer to the ignition point than the experiment inside the rig, which indicates that the flame acceleration seems to occur earlier in the simulations. The experiment and the 0.075 m grid simulation obtained their peak pressure close

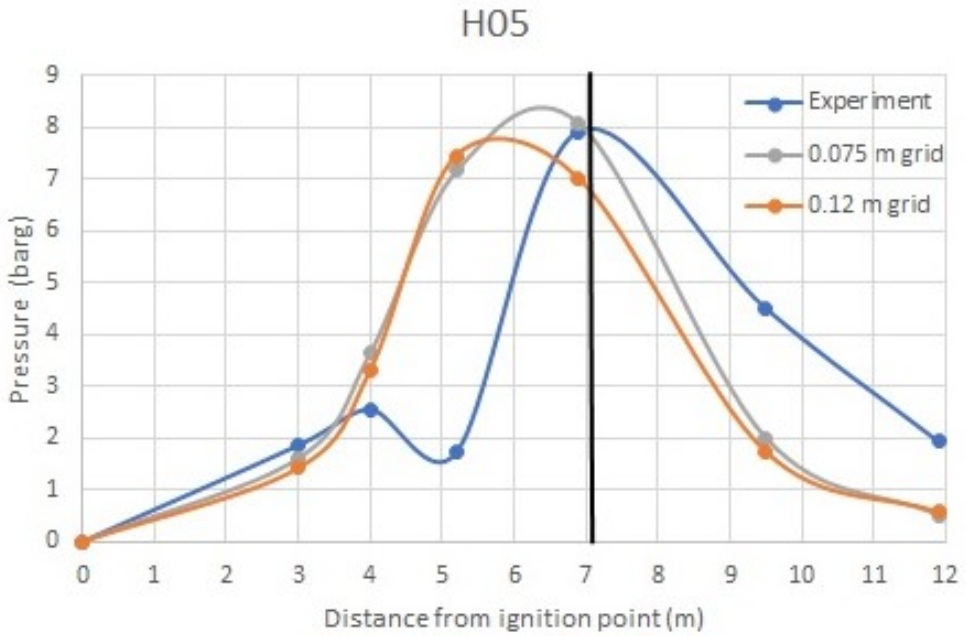

Figure 25: *Grid sensitivity for test H05 with simulations with a 0.12 m grid, 0.075 m grid resolution and the result from the experiment. The hydrogen concentration in air was 22.2 %. The black line indicates where the rig ends* [32].

to the end of the rig, around 6.9 m from the ignition point. The experiment also exhibited a decrease in overpressure between monitor points 2 and 3 (4 m - 5.2 m). BakerRisk have not commented on the reasons for this in their study.

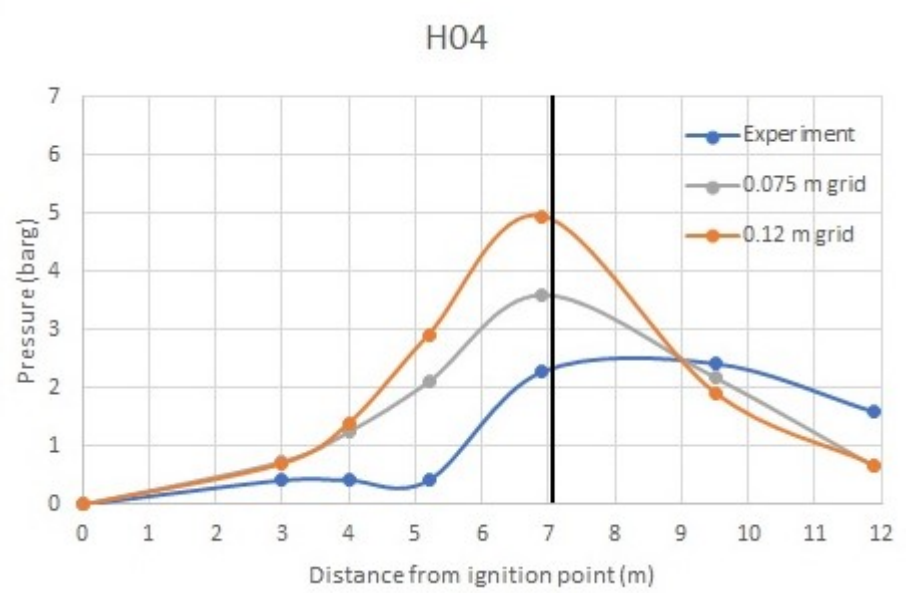

Figure 26: *Gid sensitivity of test H04 with simulations of 0.12 m grid and 0.075 m grid. The hydrogen concentration was 20.1 %. The black line indicates where the rig ends* [32].

Test H04 had a 2.1 % lower hydrogen concentration than test H05, which resulted in a considerable lower overpressure. According to figure 4, will a concentration variation of hydrogen from 22.2 % to 20.1 % decreases the burning velocity, which is corresponding to the decreased overpressure.

Figure 26 shows that the simulation overall produced higher overpressures for test H04 than observed in the experiment. The simulation with a grid resolution of 0.12 m overpredicted the maximum overpressures observed in the experiments by more than a factor 2. The simulation with a 0.075 m grid resolution predicted overpressures that were somewhat more accurate than the 0.12 m grid resolution compared to the experimental result, but still overpredicted by a factor 1.5.

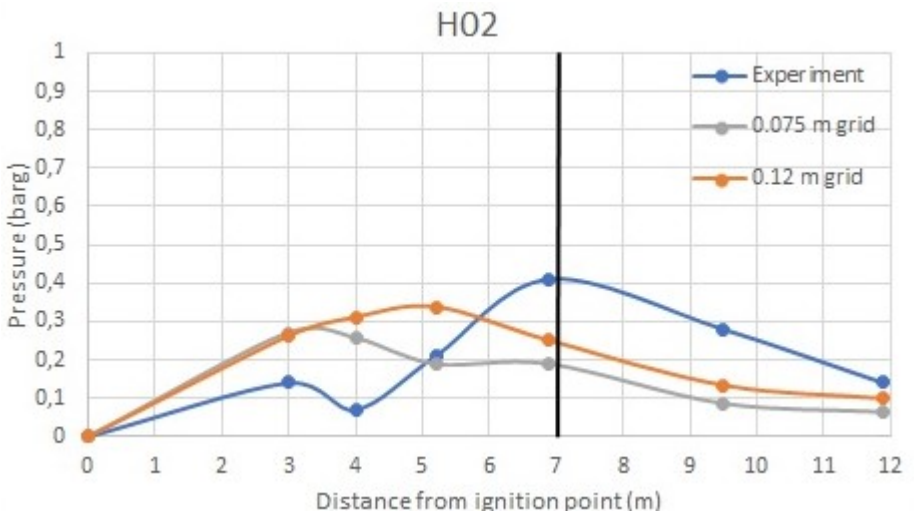

Figure 27: *Grid sensitivity of test H02 with simulations of 0.12 m and 0.075 m grid. The hydrogen concentration was 18.1 %. The black line indicates where the rig ends* [32].

Test H02 had a hydrogen concentration of 18.1 %, which was the lowest concentration of the three tests. Figure 27 shows that the simulation of H02 had a significant lower overpressure compared to test H04 and H05. By contrast with the other simulations, the overpressure in the simulation of H02 did not increase at the end of the rig. In fact, the overpressure decreased from monitor point 3 to monitor point 4 in both simulations. The experimental result of H02 seems to exhibit similar behaviour as in the previous tests, just with a lower reactivity.

Grid sensitivity

The grid resolution of 0.12 m was the coarsest recommended resolution for the geometry in the simulation, according to the guidelines in the FLACS manual. The 0.075 m grid resolution was chosen to investigate how a finer grid would impact the results. For tests H04 and H05, the 0.075 m grid simulations predicted the most accurate pressure profiles compared to the experimental results. For the test H02, the difference in the results between the two simulations were very small. Thus, the grid resolution of 0.075 m grid has been found to be the most accurate and therefore is this grid resolution used further in the validation study of the experiment from BakerRisk.

Analysis of the overpressure and potential of DDT

The maximum overpressures in the experiments increased significantly towards the end of the rig, around 7 m from the ignition point, which indicates that the flame front accelerated considerably in this region. H05, the test with the highest concentration of hydrogen (22.2 %), had a significantly higher maximum overpressure (7.93 bar) than the other tests. That is very close to the maximum overpressure from the simulation of H05 test (8.08 bar). However, the simulations predict an earlier increase in overpressure (i.e. closer to the ignition point) that observed in the experiments. This observation is the same as in validation case 1. Furthermore, the overpressure results from the simulations are clearly lower outside the rig compared to the experiments (monitor points 5 and 6). This can be due to the monitor points being in the stretched region (monitor point 5 is at the boundary of the stretched region). In general, the simulations achieved the maximum overpressure at monitor point 5 (2.44 m outside the rig) before the experiment. The figure 28 shows that the simulation of H05 is over 3 ms earlier than the experiment. In test H04 is the deviation less than 2 ms.

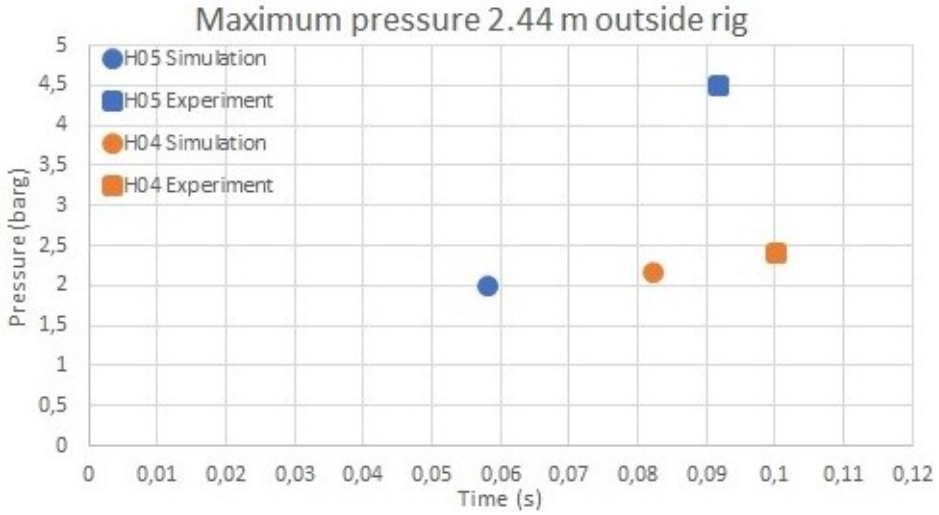

Figure 28: *Maximum pressure at monitor point 5 (9.5 m from ignition point, 2.45 m outside the rig) with test H05 (22.2% hydrogen) as blue, and the H04 (20.1% hydrogen) as orange* [32].

BakerRisk analyzed, with high speed video, that the detonation wave in test H05 traveled in approximately 1700 m/s traversing the remainder of the

Table 7: *Essential results from the experiments and the simulations [32].*

Test	Concentration (%)	Equivalence ratio	Max pressure experiment (barg)	Max pressure simulation (barg)	Max flame speed experiment (m/s)	Max flame speed simulation (m/s)
H02	18.1	0.51	0.41	0.34	-	-
H04	20.1	0.58	2.42	3.80	340	612
H05	22.2	0.66	7.93	8.08	1701	1054

mixture of hydrogen-air. Test H04 had much lower flame speed, and reached about 340 m/s. The simulation results showed that the maximum flame speed for H05 was around 1050 m/s and around 600 m/s for H04, both at monitor point 4.

Further, BakerRisk looked at the possibility of DDT in their experiments. The three first tests (H01, H02 and H04) did not show any signs of DDT. However, they could see that the blast loads were high for the H04 test. In test H05, the test with highest hydrogen concentration, DDT occurred near the end of the rig. The measured maximum pressure was around 9 bar, which is significantly higher than in the other tests. It is also possible to observe the DDT in the high-speed video of the H05 test.

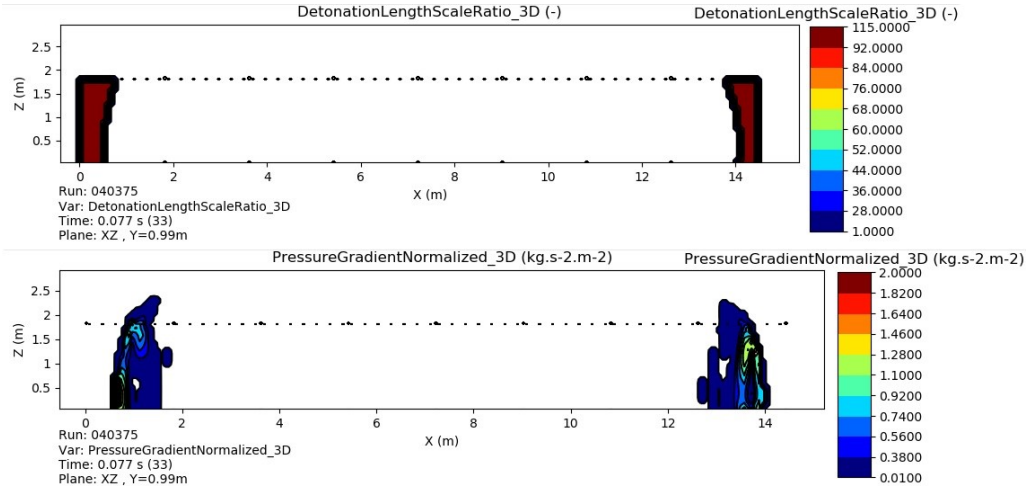

Figure 29: *Plots that indicate the DDTLS- and the DPDX-value from the H04 simulation after 0.077 s. Flame propagation is from the middle of the geometry and out on both sides.*

Figure 29 shows the partial distribution of DPDX and DDTLS in the xz-

plane for simulation H04 (20.1 % hydrogen concentration) at 0.077 s after the ignition. The figure visualizes a DPDX-value of maximum 2. The plot shows areas of green and yellow, which indicates that it reached a DPDX-value of 1.1 - 1.4. According to the FLACS User Manual, this means that a DDT is possible. Further, the DDTLS parameter has a maximum value of 115 which is significantly larger than 7, which indicates that the detonation will be able to propagate thought the rest of the gas cloud. According to figure 10, the detonation cell size (λ) in H04 would be around 60-70 mm. However, as in validation case 1, it is difficult to concluded about the DDTLS-value since the LSLIM-value in this case is complex to analyse.

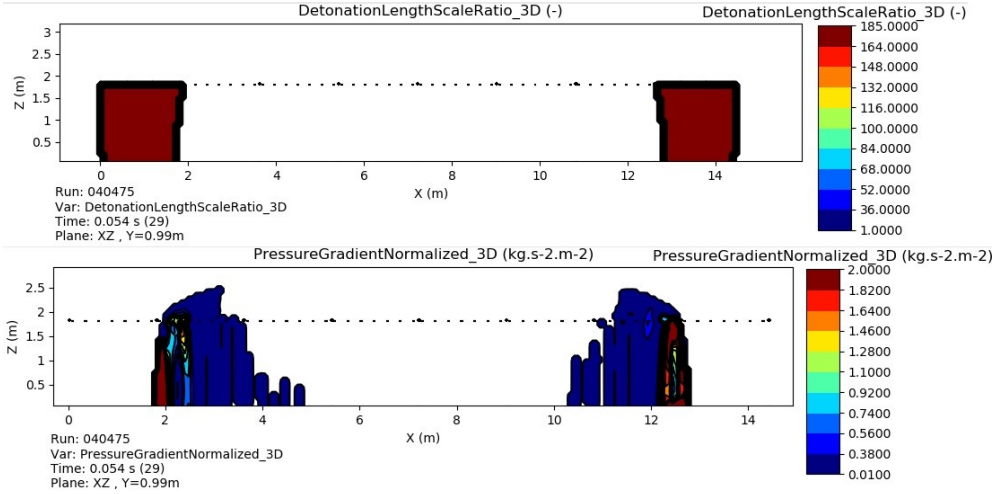

Figure 30: *Plots of DPDX- and DDTLS-value for the H05 simulation at 0.054 s. Flame propagation occurs from the middle of the geometry and towards both sides.*

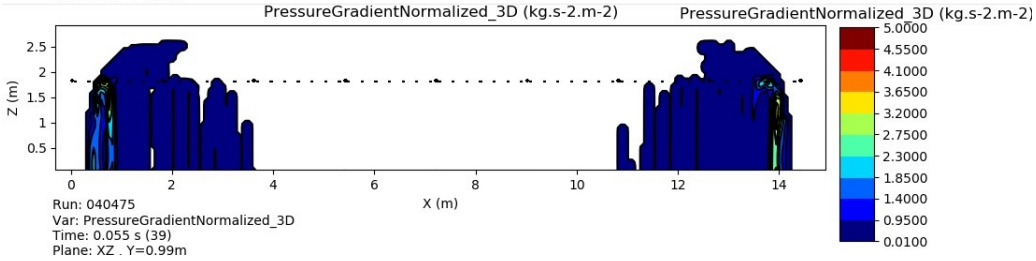

Figure 31: *Plot of DPDX-value from the H05 simulation at respectively 0.054 s and 0.055s. Flame propagation occurs from the middle of the geometry and towards both sides.*

Test H05, with the highest hydrogen concentration (22.2 %), had the clearest indication of DDT in the experimental study. The simulation of H05 shows dominant areas of red in the last 2-3 meters of the rig, when the visualization of the DPDX-value was set to maximum 2. This is illustrated in figure 30. Further, when the visualization of the DPDX-value was set to maximum 5 in figure 31, areas of yellow, green and orange were observed. This means that the DPDX-value was at least 4. However, the DDTLS-value should also be taken into account. The maximum value of the DDTLS-value was 185, which is significantly larger than 7, and exactly the same as in the simulation of H04. The detonation cell size (λ) would be around 200-300 mm. Hence, both DPDX-value and the DDTLS-value for the simulation of H05 strongly indicate that DDT will occur in this case.

Conclusions of validation case 2

- The grid sensitivity study of validation case 2 showed that the grid resolution with 0.075 m grid gave the most accurate results, especially in the test with highest hydrogen concentration (H04 and H05).
- In test H05, DDT was observed in the experiment. The simulation of H05 strongly indicated that DDT is possible/likely.
- H01, H02 and H04 did not show any sign of DDT in the experiments. However, the simulation of H04 indicated that DDT is possible.
- Possible reasons for deviations between experimental and simulated results:
  - Inaccuracies in the modelling approach.
  - Minor deviations in geometric details, due to some interpretation from the illustrations in the paper.
  - How FLACS accounts for the effect of varying concentrations on the reactivity of the mixture.

4 Accident scenarios involving releases of liquid hydrogen during bunkering operations

This chapter presents results from the simulations of the bunkering operations and investigates the overpressure and the potential of the DDT after an accidental release of liquid hydrogen. However, the chapter starts with a brief description of the large-scale release experiments which Jacobson's validated against in her thesis [12]. Further, dispersion and explosion simulations of realistic bunkering operations were completed, using settings based on the validated simulations of Jakobsen. Finally, the results from the simulations were discussed and analysed considering overpressure and DDT.

For more details about Jakobsen's results, see reference [12], and for more details about the outdoor release experiments, see references [36].

4.1 Background

In Jakobsen's thesis [12], she simulated large-scale release experiments involving liquid hydrogen. The experiments were performed for *"State Highways Authority"* and reported by the *Norwegian Defence Research Establishment (FFI)*. The purpose of the experiments was to learn more about the behavior of liquid hydrogen (LH2) during a release, which is essential information when considering the safety issues of using LH2 in the maritime sector. The first part of the experiment was an "outdoor leakage study", which was intended to simulate release of LH2 from a bunkering operation. The second part was a "closed room and ventilation mast study". The last part is not considered further in this thesis [36].

The starting point for the experiments was to simulate a realistic release scenario for a bunkering operation involving LH2. Such a case is illustrated in figure 32. In the experiments, two containers on top of each other simulated the side of a ship. According to the report, it is realistic in a maritime case to assume a leakage can occur at the side of the ship.

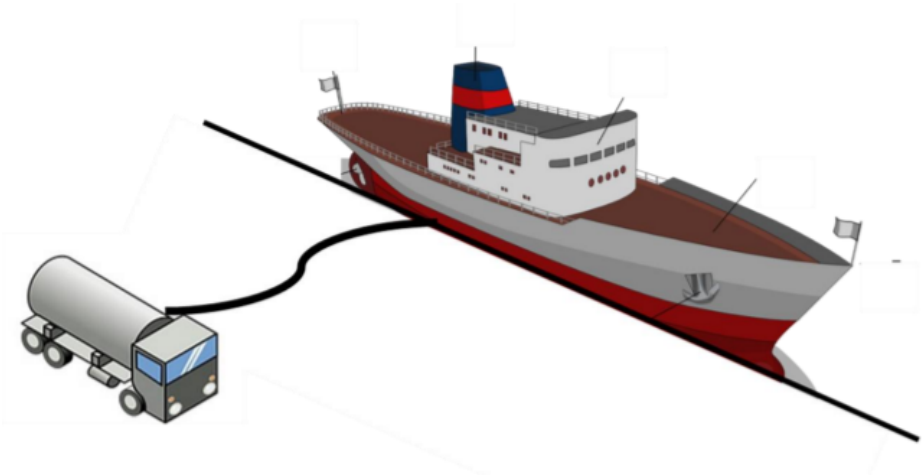

Figure 32: *Illustration of a realistic release scenario of LH2, which was the starting point for the experiments for "State Highways Authority" [36].*

Figure 33: *The experimental setup for the outdoor leakage experiments, with two containers on top of each other to simulate a shipside [36].*

Table 8: *An overview of all the tests from the outdoor release experiments [36].*

Test	Release orientation	Tanker pressure (barg)	Outflow rate (kg/s)	Ignition	Outdoor temperature (C)	Wind velocity (m/s)	Wind direction (decrees)
1	Vertical downwards (-Z)	2	0.228	No	1	3.2	246 (WSW)
2	Vertical downwards (-Z)	6	0.473	No	1.5	4.1	82 (E)
3	Vertical downwards (-Z)	10	0.730	No	2.9	5.8	259 (W)
4	Horizontal (+x)	10	0.828	No	3.3	6.7	264 (W)
5	Vertical downwards (-Z)	10	0.740	Yes	3.7	5.2	257 (W)
6	Horizontal (+x)	10	0.833	Yes	3.8	2.7	245 (WSW)
7	Vertical downwards (-Z)	0.8	0.162	No	3.2	6.5	266 (W)

In the middle of the setup, as shown in figure 33, LH2 was released through a pipe of 25.4 mm diameter. Most of the release tests had a vertically downwards release (-Z direction), but test 4 and 6 had horizontal releases (+X direction). Table 8 shows further details about the seven tests.

4.2 Methodology and setup of simulations

In the simulations of the experiments from FFI with hydrogen releases, Jakobsen [12] was able to reproduce dispersed hydrogen-air clouds that were in satisfactory agreement with the experiments. In the end of her thesis, she suggested this for further work: [12]: *"Further studies should explore more realistic conditions for bunkering operations, including conditions that may result in significant flame acceleration and DDT"*.

Hence, her set-up for releases of liquid hydrogen in FLACS was used to get valid results for the dispersion cloud in the bunkering operations in this thesis. Further, three examples of a realistic port area were created to study the potential for generating significant overpressures and DDT in regions with varying degrees of congestion. These hypothetical cases were used to simulate dispersion clouds from an accidental release of liquid hydrogen during a bunkering operation. After 60 s with continuous release of hydrogen, the clouds were ignited. Finally, the results from the explosion simulations were analysed considering the overpressure and the possibility of DDT.

Simulation set-up
The set-up for the dispersion and explosion simulations is described in the list below:

- **Geometry**: The hypothetical port area consisted of containership moored ashore, a quay, ISO-containers (standard dimensions) on the quay and the ship, tankers, a gantry crane, bunch of pallets and barrels. See figures 34, 35 and 36 for how the geometry looked in all the simulations.
- **Grid**: The grid was uniform with a resolution of 0.3 m in the core domain. The grid covered a large area in the simulations, especially in x-direction (the wind direction). Hence, the stretch domain function was used to reduce the number of grid cells. In total, the simulations had 658329 number of cells in the grid. Figure 34, 35 and 36 show the grid used in the simulations.
- **Simulation**: Maximum time for the dispersion simulations was set to 61 seconds.

- **Initial conditions**: The temperature was set to 10 C°, and the Pasquill class was set to F (stable).
- **Gas composition and volume**: The volume fraction was set to 100 % hydrogen, and the equivalence ratio was set to "1e+30".
- **Leakage**: The dispersion simulations had either a leakage in −Z-direction (vertical downwards) or +X-direction (horizontal). The outflow rate was set to 0.85 kg/s. The outlet diameter was 0.0254 m.
- **Wind**: The wind was set to blow in the +X-direction (270 °) with a velocity that varied between 5 - 8 m/s.
- **Ignition**: Time of ignition was set to 60.05 seconds for all the explosion simulations. The ignition locations varied considering where the dispersion cloud was most reactive. All the clouds were ignited at 1.5 m above the ground. The exact location for each simulation is described later in the section.

The simulations can be divided into three categories of congestion in the port area:

1. Simulations with a relatively open port area. An empty ship and a group of containers some distance away from the release point were included. Only one tanker with hydrogen was present on the quay. Case 1 and 2 were simulated with this relatively low level of congestion. Figure 34 shows how the open area was represented in FLACS.

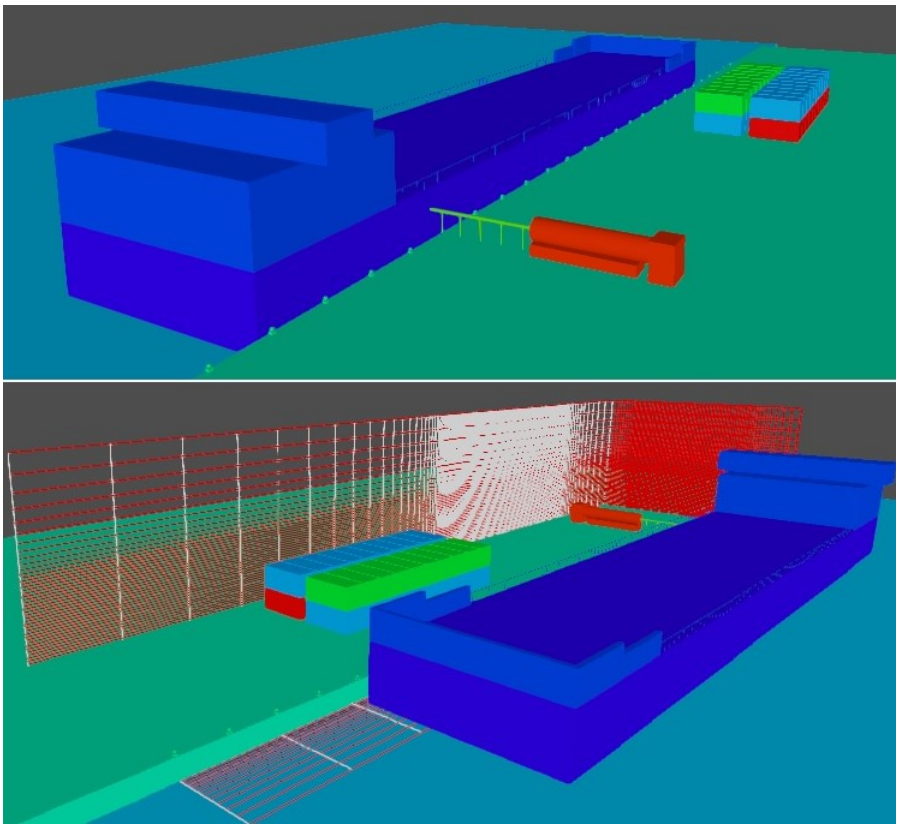

Figure 34: *Geometry and the grid for case 1 and 2 in FLACS. A ship, tanker and some containers were included.*

2. Simulations with a medium level of congestion in the port area. The ship was fully loaded with containers, and there was added one tanker with hydrogen compared to category 1. Further, the amount of containers on the quay was increased and located closer to the release point, in addition to a large gantry crane was added. See figure 35 for an overview of the port area. Case 3 and 4 were simulated with this level of congestion.

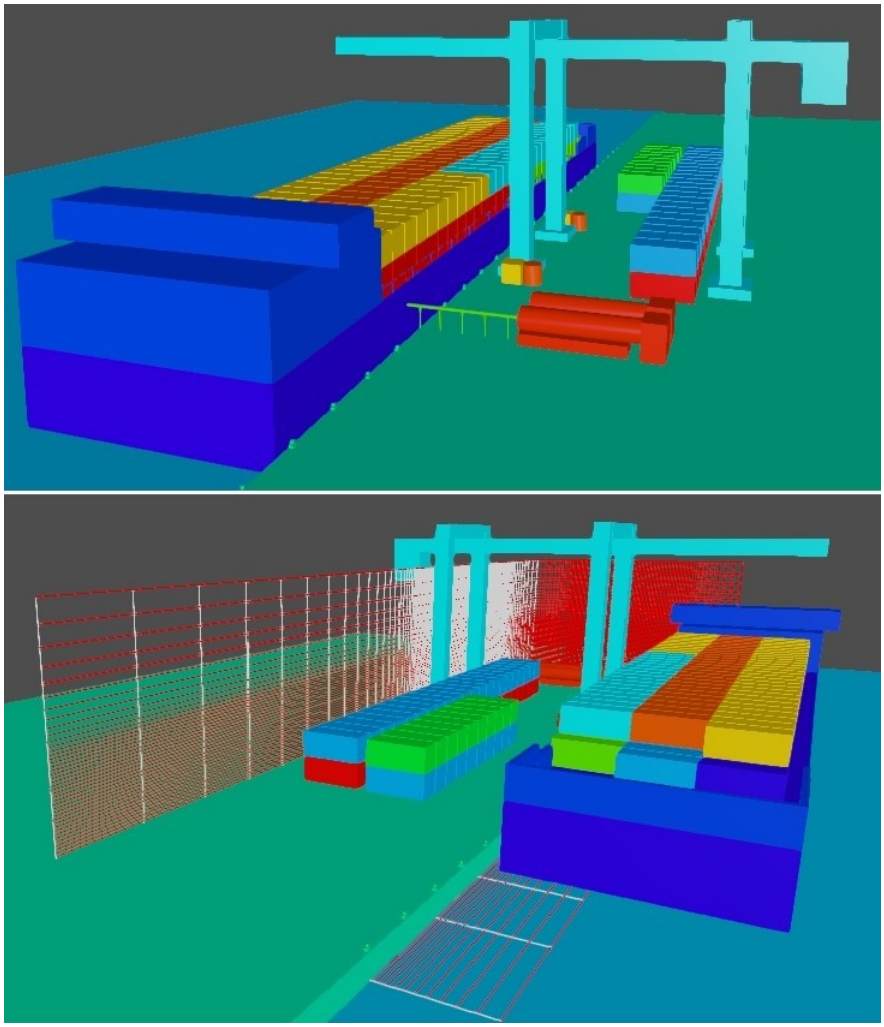

Figure 35: *Geometry and the grid for case 3 and 4 in FLACS. A fully loaded ship, two tankers, gantry crane, some obstacles and containers were included.*

3. Simulations with the highest level of congestion in the port area. As seen in figure 36, the amount of containers on the quay was increased from category 2, and they were also closer to the release point. The ship was fully loaded with containers, and two tankers with hydrogen were present on the quay. Additionally, a bunch of pallets were included and located around 10 m from the release point. Case 5 and 6 were simulated with this level of congestion.

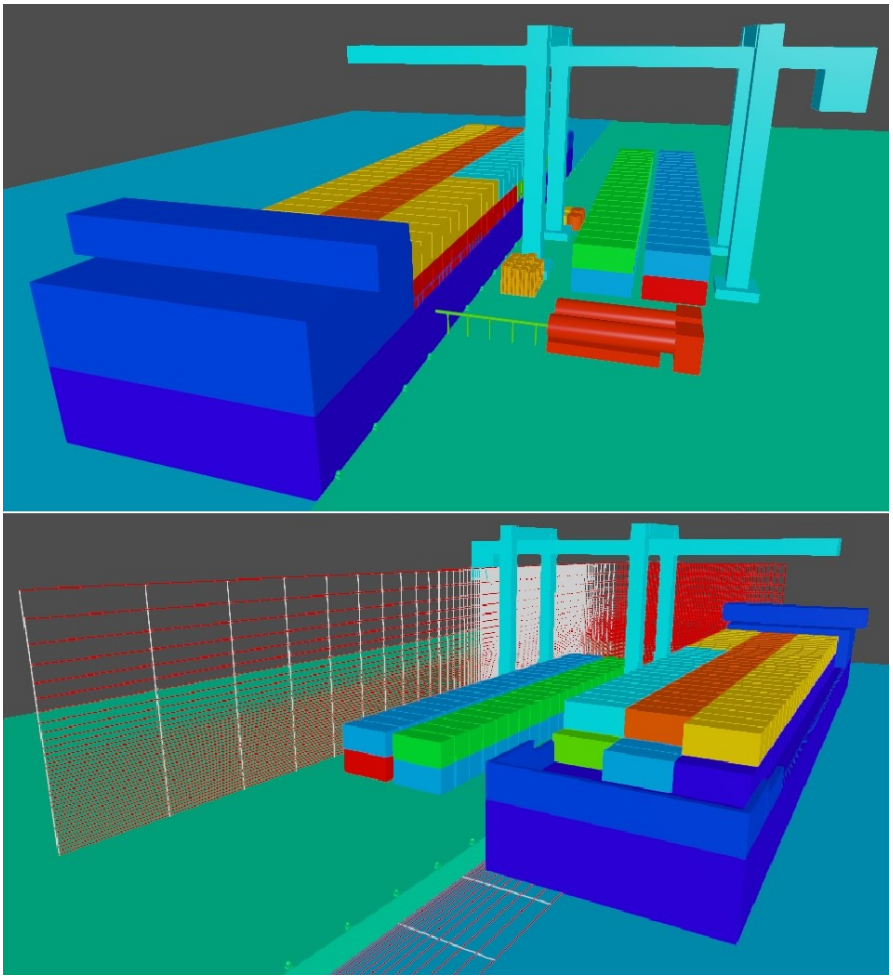

Figure 36: *Geometry and the grid for case 5 and 6 in FLACS. A fully loaded ship, two tankers, gantry crane, a bunch of pallets, some obstacles and containers were included.*

Table 9: *An overview of essential parameters in the hypothetical accident scenarios.*

Cases	Release orientation	Wind velocity (m/s)	Congestion category	Ignition point (x, y)
1	Horizontal (+X)	8	1	(-17, 18)
2	Vertical downwards (-Z)	8	1	(-22, 23.7)
3	Horizontal (+X)	8	2	(-21, 17.5)
4	Vertical downwards (-Z)	8	2	(-27, 18)
5	Horizontal (+X)	5	3	(-23.5, 18.5)
6	Vertical downwards (-Z)	5	3	(-21, 23.2)

4.3 Results and discussion

Case 1

The first case had a horizontal release (+X) in the port area with the lowest degree of congestion. Figure 34 shows how the port area was represented in FLACS. After 60 s of release, the reactive cloud was a long, outstretched cloud of about 70 m. At the widest, the cloud was about 8-10 m. Figure 37 visualises the cloud after 60 s. The ignition point was at (-17, 18), and the overpressure reached its maximum at 0.16 s after the ignition. However, in general the overpressure in case 1 was low. The maximum overpressure was 0.042 barg, as seen in figure 38.

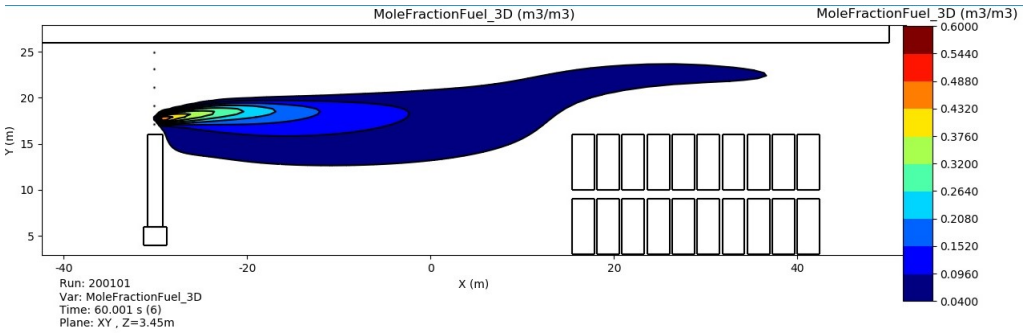

Figure 37: *The dispersion cloud from test 1 with a horizontal release after 60 s. The cloud is limited from 4 % to 60 % hydrogen.*

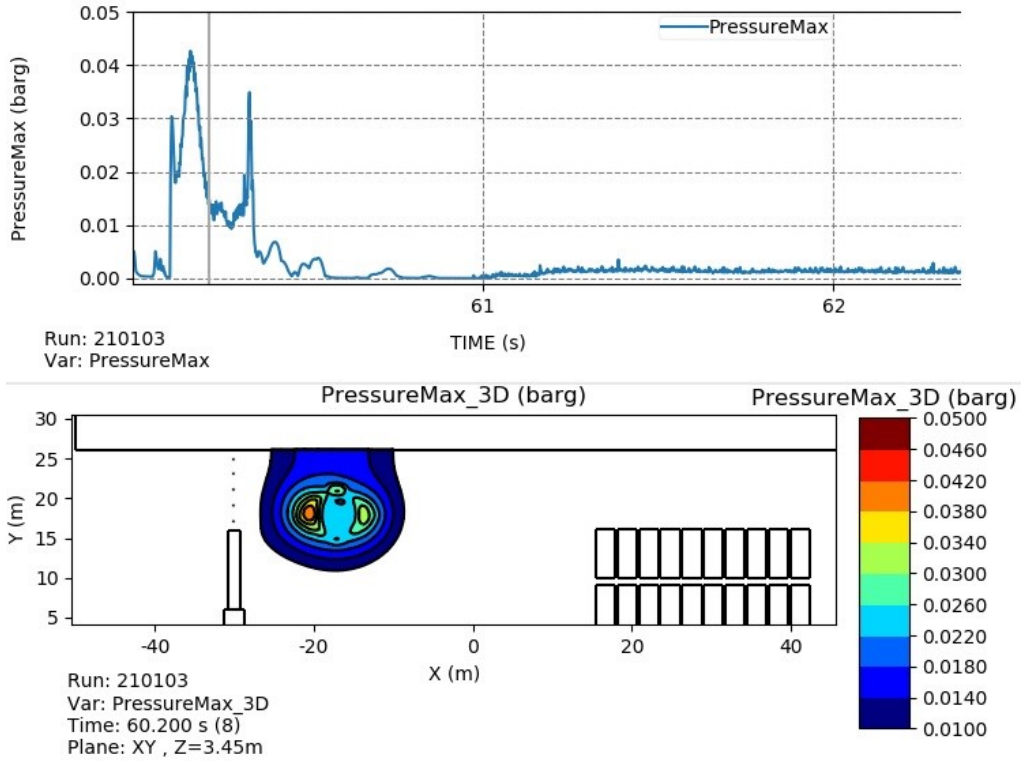

Figure 38: *The overpressure results from case 1. The top figure shows the maximum overpressure in the whole simulation domain as a function of time, the bottom shows where the maximum overpressure occurs.*

Case 2

Case 2 had the same congestion level in the port area as case 1. However, in test 2 the release direction was vertically downwards (-Z). As seen in figure 39, the dispersion cloud did not behave like the dispersion cloud in case 1. The cloud was almost split, with a reactive cloud around the tanker and a extended reactive cloud along the shipside. Figure 40 shows a maximum overpressure of 0.037 barg, which was somewhat less than that observed in case 1. The ignition point was at (-22, 23.7).

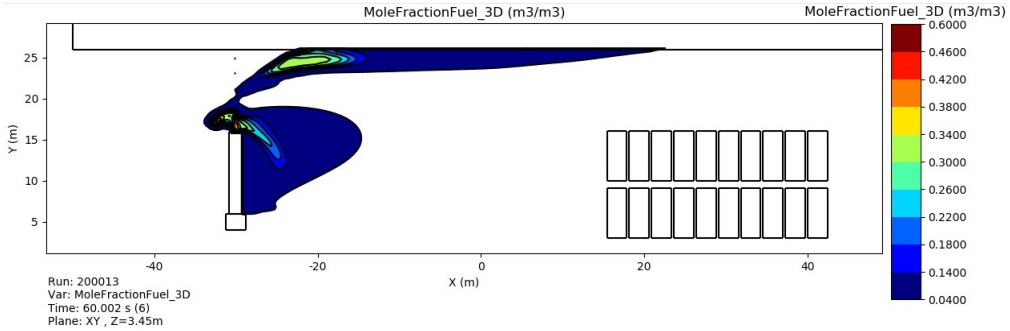

Figure 39: *The dispersion cloud from case 2 with a vertical release after 60 s. The cloud is limited from 4 % to 60 % hydrogen.*

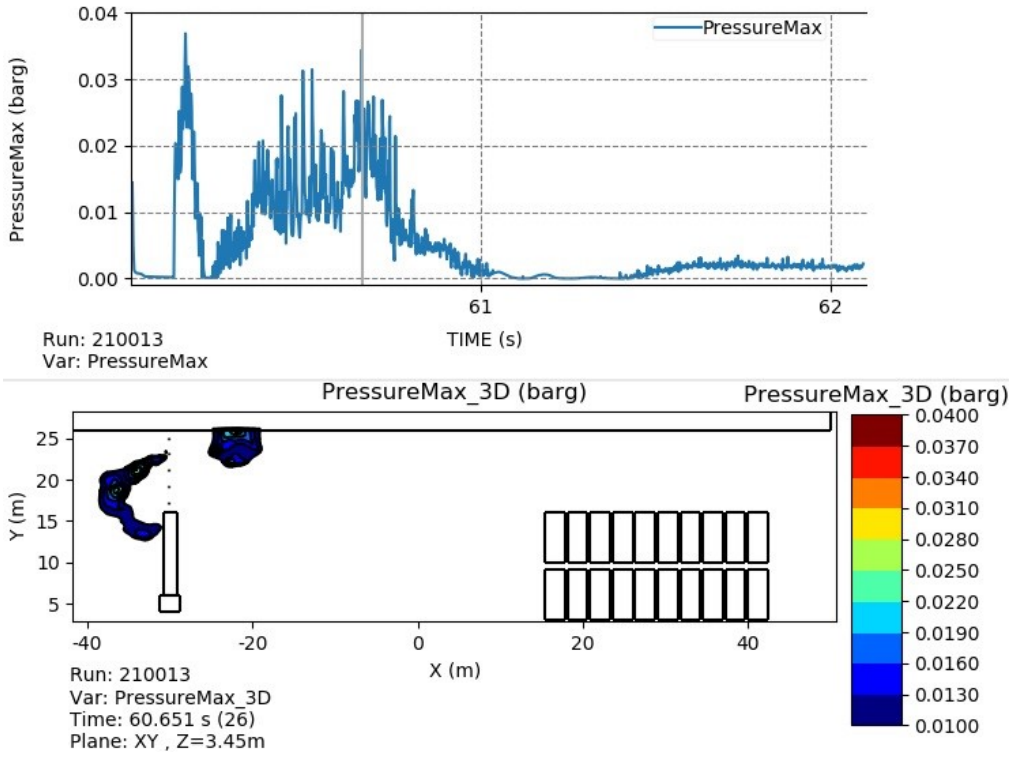

Figure 40: *The overpressure results from case 2. The top figure shows the maximum overpressure in the whole simulation domain as a function of time, the bottom shows where the maximum overpressure occurs.*

Case 3

In case 3, the congestion category was increased to medium. The port area for case 3 is shown in figure 35. The release direction was horizontal (+X), and the cloud with reactive hydrogen gas, as seen in figure 41, was not as continuous as in case 1. The ignition point was located at (-21, 17.5). According to figure 42, the maximum overpressure was 0.035 barg. The maximum overpressure occurred at 0.15 s after the ignition.

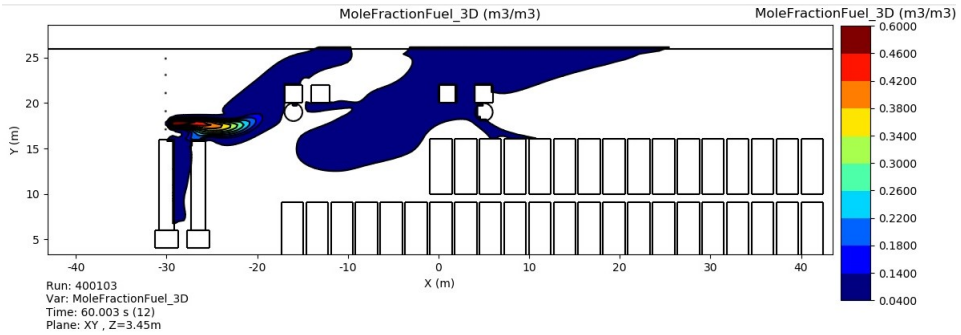

Figure 41: *The dispersion cloud from case 3 with a horizontal release after 60 s. The cloud is limited from 4 % to 60 % hydrogen.*

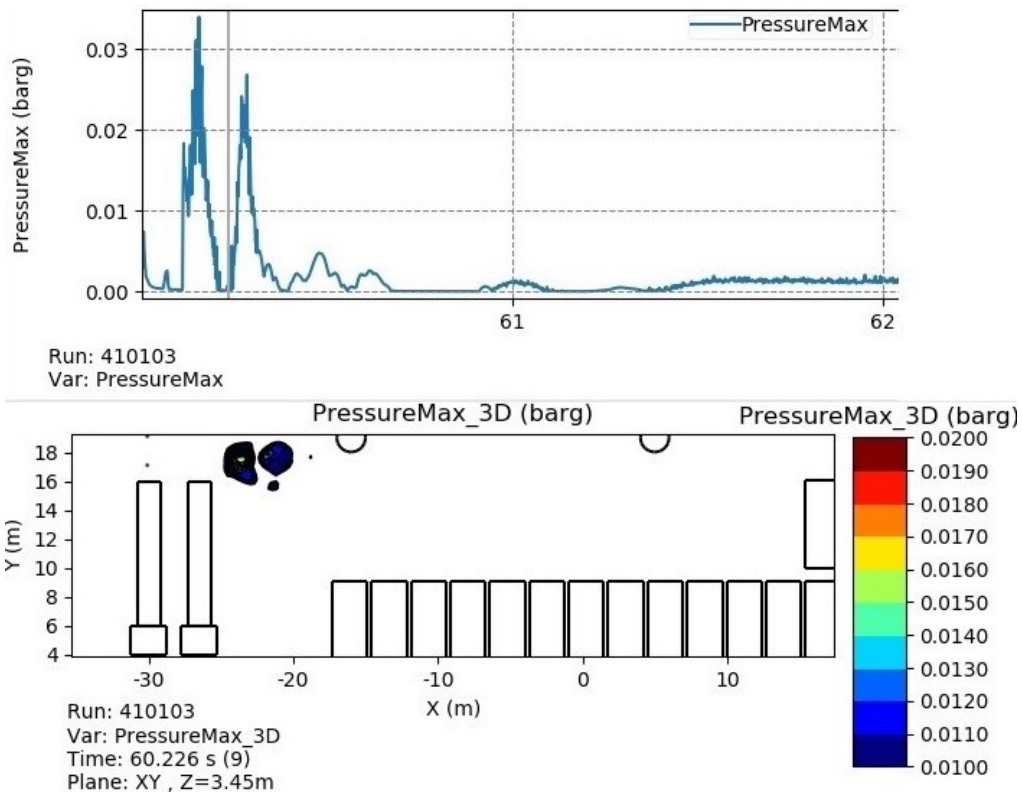

Figure 42: *The overpressure results from case 3. The top figure shows the maximum overpressure in the whole simulation domain as a function of time, the bottom shows where the maximum overpressure occurs.*

Case 4

Case 4 had a release in the vertically downwards (-Z) direction and the same port area and congestion category as case 3. As figure 43 shows, the dispersion cloud did not stretch out as much as the previous clouds. Most of the reactive gas was around the two tankers. The ignition point was located at (-27, 18). Figure 44 shows that the maximum overpressure was around 0.07 barg, reached at 0.12 s after the ignition.

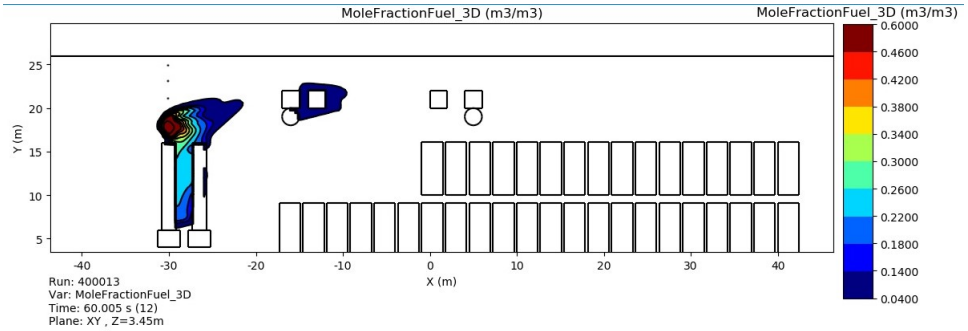

Figure 43: *The dispersion cloud from case 4 with a vertical downwards release after 60 s. The cloud is limited from 4 % to 60 % hydrogen.*

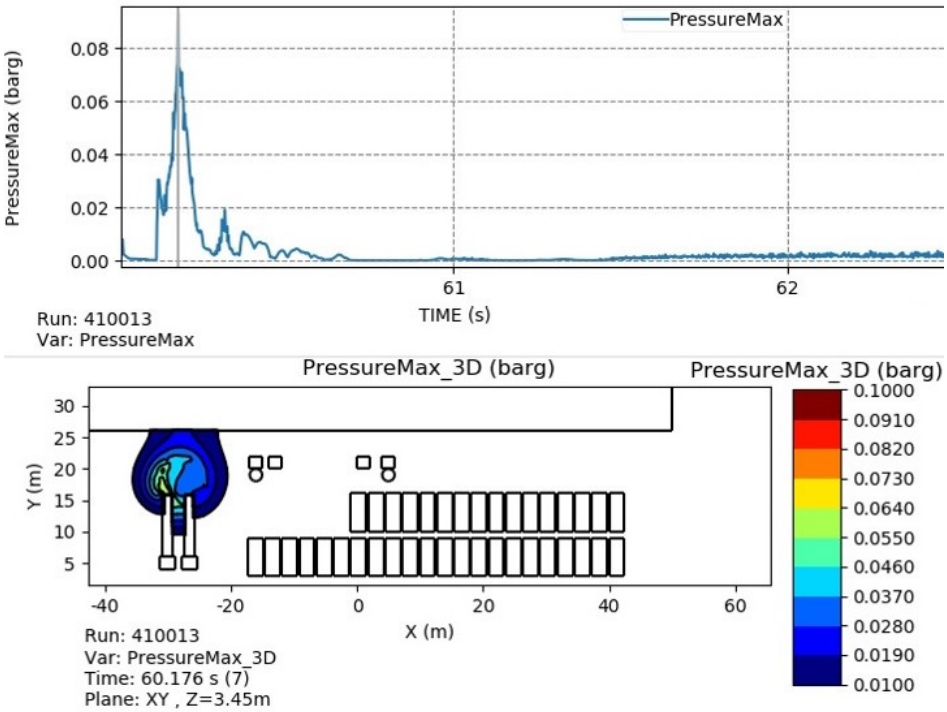

Figure 44: *The overpressure results from case 4. The top figure shows the maximum overpressure in the whole simulation domain as a function of time, the bottom shows where the maximum overpressure occurs.*

Case 5

Case 5 is the first case with the highest level of congestion in the study. In addition, the case had a lower wind velocity. See the port area in figure 36. The release direction was horizontal (+X). The dispersion cloud split, one part of the cloud extended towards the shipside and another part extended towards the containers as seen in figure 45. The ignition point was located at (-23.5, 18.5). Compared to the previous cases, case 5 reached the maximum overpressure later than observed in the other scenarios, at around 0.75 s after the ignition. The maximum overpressure was slightly higher than 0.05 barg and was reached in the area with the tankers.

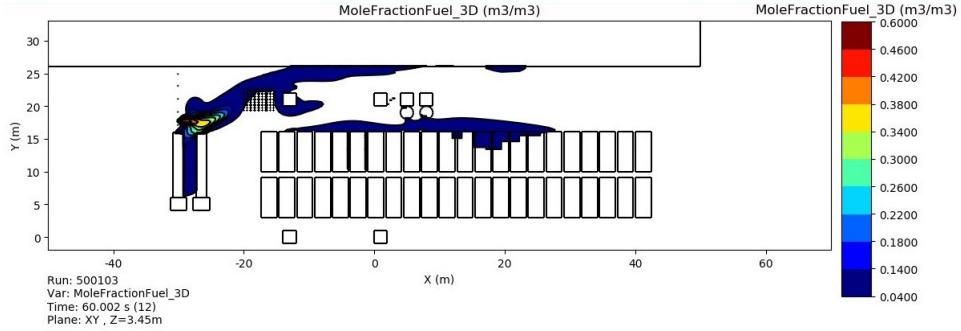

Figure 45: *The dispersion cloud from case 5 with a horizontal release after 60 s. The cloud is limited from 4 % to 60 % hydrogen.*

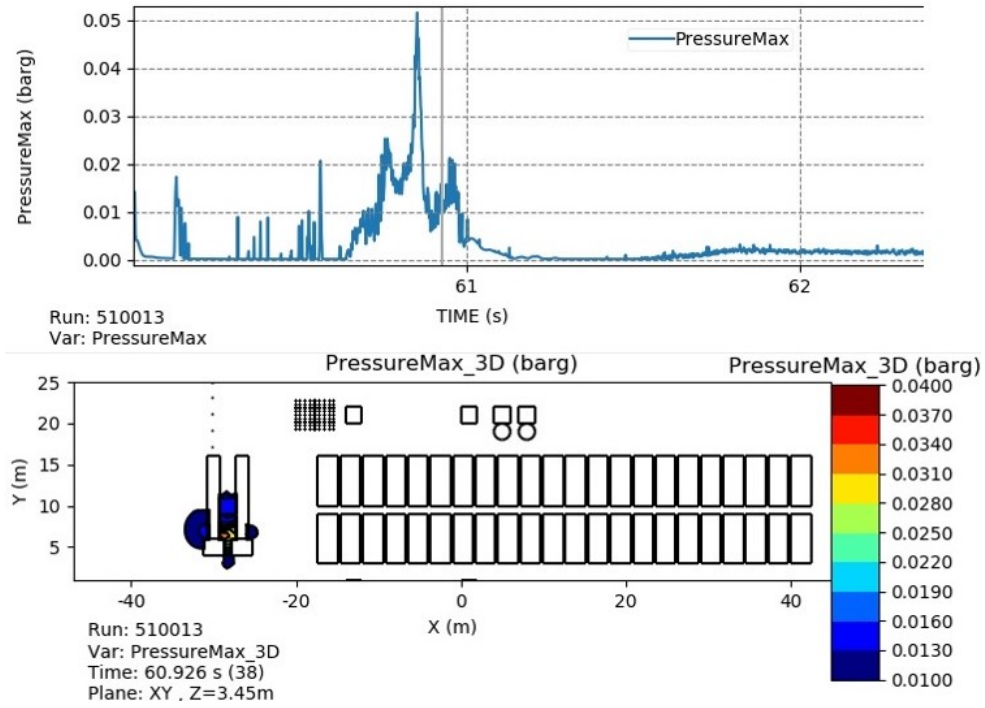

Figure 46: *The overpressure results from case 5. The top figure shows the maximum overpressure in the whole simulation domain as a function of time, the bottom shows where the maximum overpressure occurs.*

Case 6

The last case had the same port area, congestion category and wind velocity as case 5. The direction of the release was vertically downwards (-Z), and as in case 3, the cloud had the highest concentration of hydrogen between the tankers. Additionally, there was an extended reactive cloud along the shipside of around 40-50 m. The dispersion cloud is shown in figure 47. The maximum overpressure in case 6 was 0.115 barg, reached at 0.17 s after the ignition. This was the highest overpressure in all cases. As seen in figure 48, the maximum overpressure was in between the tankers on the quay. The ignition point was located at (-21, 23.2).

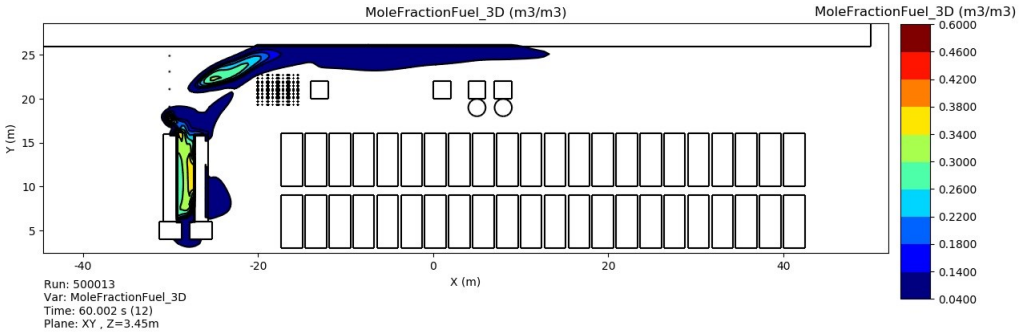

Figure 47: *The dispersion cloud from case 6 with a vertical downwards release after 60 s. The cloud is limited from 4 % to 60 % hydrogen.*

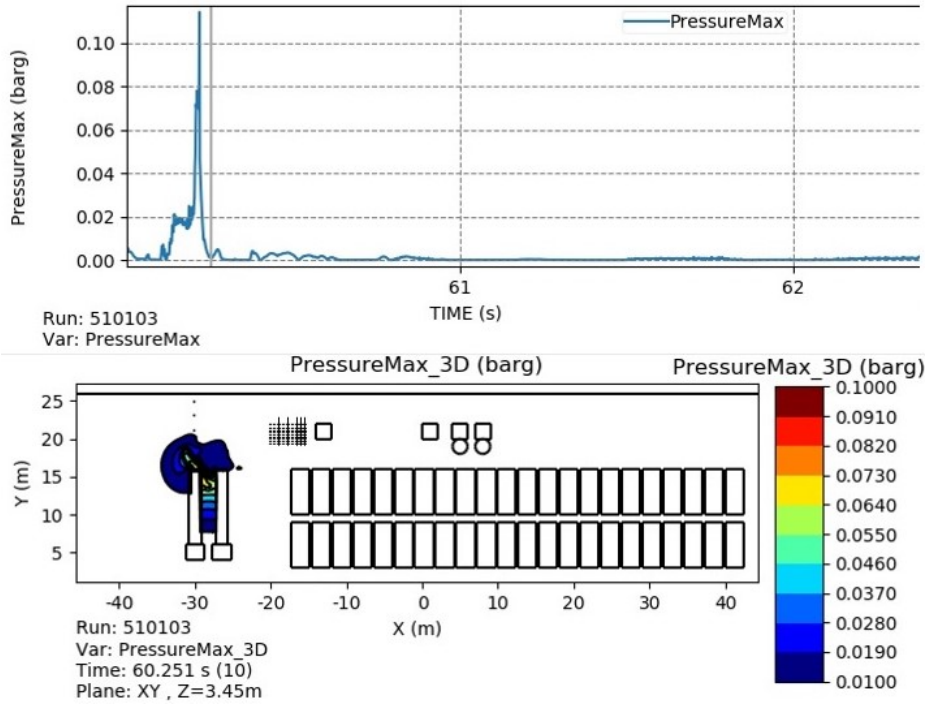

Figure 48: *The overpressure results from case 6. The top figure shows the maximum overpressure in the whole simulation domain as a function of time, the bottom shows where the maximum overpressure occurs.*

All the cases described above had the same outflow rate (0.85 kg/s), same outlet diameter (0.0254 m) and same time of release (60 s) before the ignition. In the illustrations of the dispersion clouds in all the cases, the limited boundary condition of the concentration of hydrogen was set to 4 % of hydrogen in the cloud, which is the LFL for hydrogen. However, as seen in the test results above, the dispersion clouds of reactive gas behave differently. To begin with, there was a clear difference between the clouds from a horizontal release and releases directed vertically downwards. When there was a horizontal release, the dispersion clouds extended along the shipside between 50 - 80 m. In general, the clouds were considerably more extended compared to the dispersion with releases directed vertically downwards. The figures of release in -Z direction show that the reactive clouds gathered around the tankers, close to the release point. Secondary, the obstacles in the port area for tests 3 - 6 had a significant impact on the dispersion clouds. The clouds were not extended as in tests 1 and 2, but more distributed in the port area. Additionally, tests 5 and 6 had a lower wind velocity in the simulations.

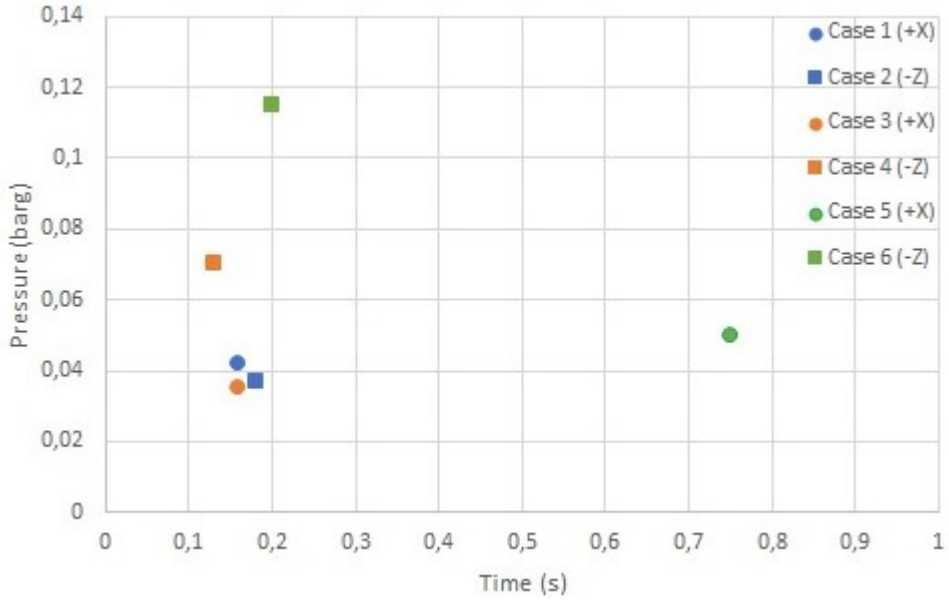

Figure 49: *Comparison of the maximum overpressure for all the cases as a function of time after ignition.*

Figure 49 illustrates the differences in maximum overpressure in the cases. In both cases 3 and 4 (congestion category 2), and cases 5 and 6 (congestion

category 3), the case with release directed vertically downwards achieved the highest maximum overpressure. Actually, the difference was up to 100 % higher maximum overpressure with releases oriented vertically downwards instead of horizontally in the direction of the wind. This can be due to the clouds are more "trapped" between the two tankers, so a more reactive cloud is generated for these cases. In cases 1 and 2, the lowest category of congestion, the maximum overpressure was roughly the same. Furthermore, the comparison of maximum overpressure shows that, in general, the maximum overpressure increased when the category of congestion in the port area increased. The exceptions were case 1 and 3, but they achieved approximately the same maximum overpressure results as the corresponding case with identical congestion category. However, in general the overpressure in all cases was very low. Case 6 achieved the highest overpressure of 0.115 barg. This is, compared to the results in the validation cases in chapter 3, a significantly lower maximum overpressure.

Furthermore, was there any sign of a DDT in the hypothetical accident scenarios? In the validation cases, DPDX and DDTLS appeared to be parameters that can indicate whether DDT could occur or not. The FLACS user manual stated that a DDT can be possible with a DPDX value between 0.5 - 2, and from possible to likely with a DPDX value above 2. The results from the tests showed that no tests achieved a DPDX value over zero. The DDTLS value over 7 indicated a easy propagation according to the FLACS user manual. The validation results showed often a significant higher value than that in the cases where DDT was likely. All the tests above achieved a DDTLS value of zero. With the results for the DPDX- and DDTLS-values, in addition to low overpressures, DDT does not appear to be likely to occur in any of the hypothetical accident scenarios investigated in this thesis.

There can be several reasons why DDT did not appear to be likely and/or high overpressure did not occur in the cases representing accidents during bunkering operations. The level of congestion in the port area is an essential parameter to achieve significant flame acceleration. As mentioned in section 4.2, the port area in the tests are just a examples of how a port area could look. Hence, there are endless ways of how a port area could appear. The three examples of port area in the cases with different categories of congestion

may have included a level of congestion (inside the most reactive parts of the clouds) that would not be able to induce sufficient flame acceleration for DDT to be possible. In cases 5 and 6, a bunch of pallets were added relatively close to the ignition point to increase the congestion, but that did not have any major impact on the overpressure. Another reason for the low overpressures obtained in the hypothetical accident scenarios could be the positioning of the ignition point. The validation cases in chapter 3 had a ignition of a hydrogen-air mixtures in a unconfined and high level of congestion area, which likely accelerated the flame and increased the overpressure. Validation case 1 also indicates that an increase in the congestion lead to an increase in the overpressure. However, there is one crucial difference between the validation cases and the bunkering operations cases. In the validation, the concentration of hydrogen was homogeneous through the cloud. This allows the flame acceleration to be continuous until it reach the end of the rig. The cloud in the bunkering operation cases was inhomogeneous.

In the hypothetical accident scenarios, the wind direction, and the release point were the same in all cases. Could the results have been differently if this was changed? For instance, if the cloud was positioned in between the ship and the quay or between containers etc, which is regions where the cloud would be more confined. According to section 2.5, a more confined area could increase the likelihood of DDT. Besides, the wind velocity was a parameter which was not the same, 5 m/s and 8 m/s, respectively. The differences in velocity did not have any crucial impact on how the clouds developed. This may be a results of too low velocities. Could a higher velocity have another impact of the overpressure? Since a higher velocity of the wind would have increased the inital turbulence, which is crucial for the flame acceleration, or could a higher win speed lead to a more rapid dispersion of the cloud to lower concentrations. In addition, the initial turbulence could also have been created if the jet release was directed into a congested region.

Further, validation case 2 in section 3.2 indicated that the concentration of hydrogen in the ignited cloud is essential for high maximum overpressure and for the possibility of DDT. Figure 7 shows that the simulation of the test with lowest concentration of hydrogen (18.1 % hydrogen) achieved a maximum overpressure of 0.34 barg. The simulation with 20.1 % hydrogen

achieved a maximum overpressure close to 4 barg, and the simulation with 22.2 % hydrogen achieved a maximum overpressure above 8 barg. In addition, the test with highest concentration of hydrogen indicated that DDT was possible/likely. Hence, hydrogen concentration affects how reactive the cloud is, and the validation case 2 indicates that a concentration of hydrogen above 20 % in a cloud is much more reactive than a cloud below 20 '%. The dispersion simulations of the hypothetical accident scenarios shows that there were areas in the clouds where the concentration of hydrogen was up to 60 %. However, these areas were just a small part of the cloud. The concentration of hydrogen was below 20 % in most of the clouds. This indicates that the reactivity of the clouds was not sufficient to achieve higher overpressure and possibility of DDT.

However, in the cases with hypothetical accident scenarios, higher overpressures and a higher likelihood of DDT might have been obtained with more congestion present in the most reactive region of the cloud, closer to the ignition point.

5 Conclusions

The main focus in this thesis was to analyse the applicability of the CFD tool FLACS to predict the flame acceleration through large-scale, unconfined, flammable clouds with hydrogen-air mixture, and investigate the overpressure and the possibility of DDT in cases where there was a accidental release of hydrogen in a bunkering operations. This chapter presents the conclusions and suggestions for further work.

5.1 Main conclusions

A list of conclusions from the results and discussion in chapter 3 and 4:

- In the hypothetical accident scenarios of hydrogen releases in the port area, all the cases achieved low overpressure. The cases with release directed vertically downwards achieved in general higher overpressure compared to the cases with release horizontal. Furthermore, none of the cases showed any sign of DDT.
- However, the number of investigated scenarios in the present work was limited, so this is not necessarily a general conclusion. Higher overpressures and a higher likelihood of DDT might have been obtained with more congestion present in the most reactive region of the cloud, closer to the ignition point.
- The validation of FLACS against unconfined and large-scale experiments with hydrogen-air mixtures showed that FLACS predicted the overpressure and the possibility of DDT relatively accurately. However, the flame acceleration process in the experiments was not exactly reproduced in the simulations.
- Validation case 2 indicated that the concentration level of hydrogen in air is crucial for the reactivity of the cloud. The clouds with 20 % hydrogen, or above, achieved significantly higher flame acceleration and overpressure. Furthermore, to obtain high overpressures and DDT, a sufficiently reactive cloud must be present in an extended region, to allow for continuous flame acceleration in that region.

- The grid sensitivity study of the validation cases showed that the largest recommended grid resolution resulted in the most accurate results for the experiments with the lowest congestion level. When the congestion level was increased, a finer grid gave the most accurate results.

5.2 Suggestions for further work

The list below presents future improvements on the present work and recommendations for future studies based on this thesis:

- Investigate the effect of changes in the port area considering the possibility of DDT. Could an area with a higher level of congestion or/and confinement increase the likelihood of DDT? For instance, more pallets and containers closer to the ignition point. Furthermore, look into how to achieve the most reactive gas cloud of a accidental release of hydrogen in the port area, including varied setup of wind velocity, release direction and release point.
- Search for and include additional relevant validation cases.
- Explore whether the consequences of a DDT can be represented in FLACS, for example applying the approach by Hansen & Johnson (2015) [37].
- Further develop and refine the criterion for likelihood of DDT developing in FLACS, exploring the findings regarding the critical cell size gradient for the propagation of a detonation from Bauwens & Dorofeev (2020) [38] and the explosion length as a measure of detonability from Radulescu (2022) [39].
- Investigate the effect of heat transfer from liquid hydrogen (LH2) to the surroundings, in addition to the condensation of the ambient air.

References

[1] O. R. Hansen, *Hydrogen safety: Kjørbo incident, overview and perspectives*, 2019. [Online]. Available: https://mozees.no/wp-content/uploads/2019/10/Hansen_Hydrogen-safety_Kjoerbo-incident-overview-and-perspectives.pdf.

[2] U. N. UN). "What do we need to achieve at cop26?" (2021), [Online]. Available: https://ukcop26.org/cop26-goals/.

[3] H. Council, "Hydrogen for net zero-a critical cost-competitive energy vector," 2021.

[4] I. E. A. (IEA), ""world energy outlook 2019"." [Online]. Available: https://www.iea.org/reports/world-energy-outlook-2019.

[5] I. M. O. (IMO). "Imo and the sustainable development goals." (2019), [Online]. Available: https://www.imo.org/en/MediaCentre/HotTopics/Pages/SustainableDevelopmentGoals.aspx.

[6] M. Pagliaro and A. Iulianelli, "Hydrogen refueling stations: Safety and sustainability," *General Chemistry*, vol. 6, no. 1, p. 190 029, 2020.

[7] I. M. O. (IMO=, *International code of safety for ships using gases or other low-flashpoint fuels (igf code)*, 2016.

[8] T. Skjold, H. Hisken, L. Bernard, *et al.*, "Blind-prediction: Estimating the consequences of vented hydrogen deflagrations for inhomogeneous mixtures in 20-foot iso containers," *Journal of Loss Prevention in the Process Industries*, vol. 61, pp. 220–236, 2019.

[9] T. Skjold, "Flame propagation in dust clouds. numerical simulation and experimental investigation," 2014.

[10] A. Neville, "Lessons learned from a hydrogen explosion," *Power (New York)*, vol. 153, no. 5, 2009.

[11] "Hydrogen safety systems operated effectively, prevented injury at plant explosion." (2020), [Online]. Available: https://www.oneh2.com/assets/images/Final%5C%20OneH2%5C%20news%5C%20release_2.pdf.

[12] J. C. Jakobsen, "Towards a regulatory framework for the use of liquid hydrogen as a fuel for ships: Critical analysis of the prescriptive requirements for bunkering operations," M.S. thesis, The University of Bergen, 2021.

[13] R. Eckhoff, *Explosion hazards in the process industries*. Gulf Professional Publishing, 2016, pp. 2–15.

[14] L. Klebanoff, J. Pratt, and C. LaFleur, "Comparison of the safety-related physical and combustion properties of liquid hydrogen and liquid natural gas in the context of the sf-breeze high-speed fuel-cell ferry,"

International Journal of Hydrogen Energy, vol. 42, no. 1, pp. 757–774, 2017.

[15] F. Birol, "The future of hydrogen: Seizing today's opportunities," *IEA Report prepared for the G*, vol. 20, 2019.

[16] O. R. Hansen, "Liquid hydrogen releases show dense gas behavior," *International Journal of Hydrogen Energy*, vol. 45, no. 2, pp. 1343–1358, 2020.

[17] A. A. Konnov, A. Mohammad, V. R. Kishore, N. I. Kim, C. Prathap, and S. Kumar, "A comprehensive review of measurements and data analysis of laminar burning velocities for various fuel+ air mixtures," *Progress in Energy and Combustion Science*, vol. 68, pp. 197–267, 2018.

[18] E. S. Oran, G. Chamberlain, and A. Pekalski, "Mechanisms and occurrence of detonations in vapor cloud explosions," *Progress in Energy and Combustion Science*, vol. 77, p. 100 804, 2020.

[19] D. A. Crowl and Y.-D. Jo, "The hazards and risks of hydrogen," *Journal of Loss Prevention in the Process Industries*, vol. 20, no. 2, pp. 158–164, 2007.

[20] D. Jamois, C. Proust, J. Hebrard, *et al.*, "Turbulence in real flammable gas releases," in *13th International symposium on hazards, prevention, and mitigation of industrial explosions (ISHPMIE)*, 2020.

[21] R. King, "Introduction," in *Safety in the Process Industries*, R. King, Ed., Butterworth-Heinemann, 1990, pp. 1–5, ISBN: 978-0-7506-1019-3. DOI: https://doi.org/10.1016/B978-0-7506-1019-3.50007-5. [Online]. Available: https://www.sciencedirect.com/science/article/pii/B9780750610193500075.

[22] P. Middha, "Development, use, and validation of the cfd tool flacs for hydrogen safety studies," 2010.

[23] D. B. Spalding, B. Launder, A. Morse, and G. Maples, "Combustion of hydrogen-air jets in local chemical equilibrium: A guide to the charnal computer program," Tech. Rep., 1974.

[24] H. Hisken, "Investigation of instability and turbulence effects on gas explosions: Experiments and modelling," 2018.

[25] Gexcon, *"flacs-cfd v21.1 user's manual"*, 2021.

[26] G. Ciccarelli and S. Dorofeev, "Flame acceleration and transition to detonation in ducts," *Progress in energy and combustion science*, vol. 34, no. 4, pp. 499–550, 2008.

[27] B. J. Arntzen, "Modelling of turbulence and combustion for simulation of gas explosions in complex geometries," 1998.

[28] K. van Wingerden, D. Bjerketvedt, and J. R. Bakke, "Detonations in pipes and in the open," in *Paper in Proceedings of the Petro-Chemical Congress (June 23–24, 1999)*, Citeseer, 1999, p. 15.

[29] P. Middha and O. R. Hansen, "Predicting deflagration to detonation transition in hydrogen explosions," *Process Safety Progress*, vol. 27, no. 3, pp. 192–204, 2008.

[30] M. Ivings, C. Lea, D. Webber, S. Jagger, and S. Coldrick, "A protocol for the evaluation of lng vapour dispersion models," *Journal of Loss Prevention in the Process Industries*, vol. 26, no. 1, pp. 153–163, 2013.

[31] T. Skjold, V. Wingerden, I. Storvik, *et al.*, "Final report "jip flacs 2011 and beyond"," 2013.

[32] L. Shirvill, T. Roberts, M. Royle, D. Willoughby, and P. Sathiah, "Experimental study of hydrogen explosion in repeated pipe congestion–part 1: Effects of increase in congestion," *International Journal of Hydrogen Energy*, vol. 44, no. 18, pp. 9466–9483, 2019.

[33] J. Thomas and D. Malik, "Ammonia and hydrogen vapor cloud explosion testing (a tale of two gases)," *Baker Enrgineering and Risk consultants*, pp. 269–280, 2017.

[34] L. Shirvill, T. Roberts, M. Royle, D. Willoughby, and P. Sathiah, "Experimental study of hydrogen explosion in repeated pipe congestion–part 2: Effects of increase in hydrogen concentration in hydrogen-methane-air mixture," *International Journal of Hydrogen Energy*, vol. 44, no. 5, pp. 3264–3276, 2019.

[35] S. Lakshmipathy, T. Skjold, H. Hisken, and G. Atanga, "Consequence models for vented hydrogen deflagrations: Cfd vs. engineering models," *International Journal of Hydrogen Energy*, vol. 44, no. 17, pp. 8699–8710, 2019.

[36] J. Aaneby, T. Gjesdal, and Ø. A. Voie, "Large scale leakage of liquid hydrogen (lh2)–tests related to bunkering and maritime use of liquid hydrogen," 2021.

[37] O. R. Hansen and D. M. Johnson, "Improved far-field blast predictions from fast deflagrations, ddts and detonations of vapour clouds using flacs cfd," *Journal of Loss Prevention in the Process Industries*, vol. 35, pp. 293–306, 2015.

[38] C. R. L. Bauwens and S. B. Dorofeev, "Modeling detonation limits for arbitrary non-uniform concentration distributions in fuel–air mixtures," *Combustion and Flame*, vol. 221, pp. 338–345, 2020.

[39] M. P. A. Radulescu and F. Zangene, "The explosion length as a measure of detonability: Review of data in methane and hydrogen," 2022.